

Understanding controls on rapid ice-stream retreat during the last deglaciation of Marguerite Bay, Antarctica, using a numerical model

Stewart S. R. Jamieson,¹ Andreas Vieli,^{1,2} Colm Ó Cofaigh,¹ Chris R. Stokes,¹ Stephen J. Livingstone,³ and Claus-Dieter Hillenbrand⁴

Received 26 July 2013; revised 8 November 2013; accepted 18 November 2013; published 18 February 2014.

[1] Using a one-dimensional numerical model of ice-stream flow with robust grounding-line dynamics, we explore controls on paleo-ice-stream retreat in Marguerite Bay, Antarctica, during the last deglaciation. Landforms on the continental shelf constrain the numerical model and suggest that retreat was rapid but punctuated by a series of slowdowns. We investigate the sensitivity of ice-stream retreat to changes in subglacial and lateral topography and to forcing processes including sea-level rise, enhanced melting beneath an ice shelf, atmospheric warming, and ice-shelf debudding. Our experiments consistently reproduce punctuated retreat on a bed that deepens inland, with retreat-rate slowdowns controlled by narrowings in the topography. Sensitivity experiments indicate that the magnitudes of change required for individual forcing mechanisms to initiate retreat are unrealistically high but that thresholds are reduced when processes act in combination. The ice stream is, however, most sensitive to ocean warming and associated ice-shelf melting, and retreat was most likely in response to external forcing that endured throughout the period of retreat rather than to a single triggering “event.” Timescales of retreat are further controlled by the delivery of ice from upstream of the grounding line. Due to the influence of topography, modeled retreat patterns are insensitive to the temporal pattern of forcing evolution. We therefore suggest that despite regionally similar forcing mechanisms, landscape controls significant contrasts in retreat behavior between adjacent but topographically distinct catchments. Patterns of ice-stream retreat in the past, present, and future should therefore be expected to vary significantly.

Citation: Jamieson, S. S. R., A. Vieli, C. Ó Cofaigh, C. R. Stokes, S. J. Livingstone, and C.-D. Hillenbrand (2014), Understanding controls on rapid ice-stream retreat during the last deglaciation of Marguerite Bay, Antarctica, using a numerical model, *J. Geophys. Res. Earth Surf.*, 119, 247–263, doi:10.1002/2013JF002934.

1. Introduction

[2] Ice streams are rapidly flowing ($> 1 \text{ km yr}^{-1}$) components of ice sheets which extend for hundreds of kilometers and drain significant portions of their mass [Bamber *et al.*, 2000], thereby directly influencing sea level. Observations of modern ice streams in Greenland and Antarctica demonstrate that they are highly dynamic features where changes in flow speed and configuration can occur over a wide range of temporal (hours to

millennia) and spatial (tens of m to hundreds km) scales [Anandakrishnan and Alley, 1997; Fahnestock *et al.*, 2000; Jacobel *et al.*, 2000; Joughin *et al.*, 2002; Anandakrishnan *et al.*, 2003; Joughin *et al.*, 2003; Siegert *et al.*, 2003]. The key to predicting marine ice-stream behavior, and in particular the movement of their grounding lines (the transition between grounded and floating ice), lies in understanding their sensitivity to external forcings and to localized factors which may modulate their subsequent responses. In this paper, we aim to determine the controls on the long-term retreat behavior of the marine-based Marguerite Bay paleo-ice stream (MBIS) during the last deglaciation of the Antarctic Peninsula.

[3] A number of external forcing mechanisms may drive marine ice-stream retreat. Of these, ocean-driven melting, whereby relatively warm sea water melts the underside of ice shelves, seems arguably the most important because it can reduce their buttressing effect, promote grounding-line retreat, and drive dynamic thinning through the accelerated drawdown of ice from significant distances upstream [Payne *et al.*, 2004; Shepherd *et al.*, 2004; Price *et al.*, 2008; Pritchard *et al.*, 2009; Gladstone *et al.*, 2012]. Climate influences ice streams through accumulation and ablation patterns, ice temperature, and therefore hydraulic conditions and

Additional supporting information may be found in the online version of this article.

¹Department of Geography, Durham University, Durham, UK.

²Department of Geography, University of Zurich, Zurich, Switzerland.

³Department of Geography, University of Sheffield, Sheffield, UK.

⁴British Antarctic Survey, Cambridge, UK.

Corresponding author: S. S. R. Jamieson, Department of Geography, Durham University, South Rd., Durham DH1 3LE, UK. (Stewart.Jamieson@durham.ac.uk)

©2013. The Authors.

This is an open access article under the terms of the Creative Commons Attribution License, which permits use, distribution and reproduction in any medium, provided the original work is properly cited. 2169-9003/14/10.1002/2013JF002934

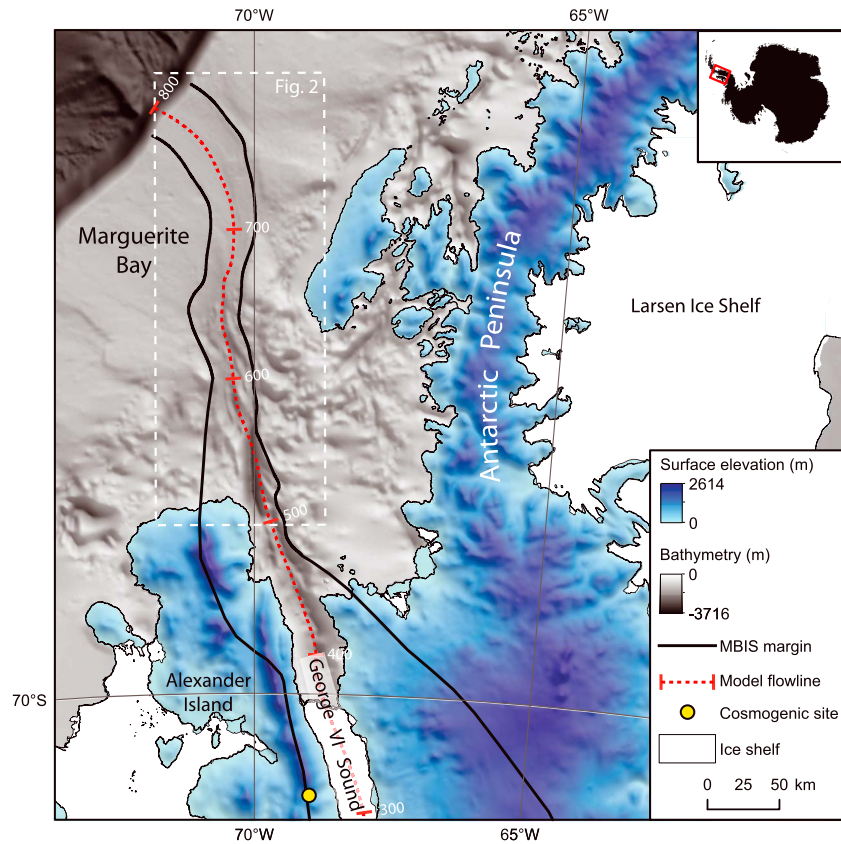


Figure 1. Marguerite Bay and the topographic and bathymetric setting of the paleo-ice stream. The MBIS flowed from George VI Sound to the continental shelf edge along the red dashed center line (intervals correspond to 100 km spacing in model output figures). The lateral margins of the ice stream (fast flow) are indicated by the thick black lines. Surface elevation and bathymetry data are from BEDMAP2 [Fretwell *et al.*, 2013], and the cosmogenic exposure age site is from Bentley *et al.* [2006].

calving processes [Benn *et al.*, 2007; Nick *et al.*, 2010]. Sea level directly affects flotation and the hydrostatic back pressure of the water body upon the face of the ice-stream terminus [Hindmarsh, 2006].

[4] However, local or internal factors can modulate the pattern of grounding-line retreat. In general, ice discharge at the grounding line increases with water depth [Weertman, 1974; Thomas and Bentley, 1978; Schoof, 2007] and is therefore controlled by topography [Powell, 1991; Ó Cofaigh *et al.*, 2008; Briner *et al.*, 2009; Durand *et al.*, 2011]. As a consequence, and in the absence of an ice shelf, subglacial beds that deepen inland can enhance the likelihood of unstable retreat, generating a potential “marine ice-sheet instability” [Weertman, 1974; Thomas and Bentley, 1978; Schoof, 2007], while local areas of high relief provide pinning points for grounding-line stabilization. Lateral constrictions in the width of an ice stream or outlet glacier trough can also slow retreat rates by enhancing drag on the trough sides [Whillans and van der Veen, 1997; O’Neel *et al.*, 2005; Jamieson *et al.*, 2012; Carr *et al.*, 2013; Enderlin *et al.*, 2013a; Nick *et al.*, 2013]. Ice shelves can locally provide additional buttressing to the grounding line via lateral stresses [Thomas, 1979; Dupont and Alley, 2005] to the extent that grounding-line stability is possible on a reverse-sloping bed [Goldberg *et al.*, 2009; Gudmundsson *et al.*, 2012; Gudmundsson, 2013]. Finally, basal sediment conditions, which are important for ice-stream flow in regions like West Antarctica, evolve in

response to changes in the overlying ice configuration and to changing hydraulic conditions and temperatures at the bed [Alley *et al.*, 1986; Anandakrishnan and Alley, 1997; Bougamont *et al.*, 2003; Alley *et al.*, 2007].

[5] These external forcings and internal factors are often linked, with feedbacks occurring between them. The complex and nonlinear nature of these feedbacks suggests that the contemporary observational record spanning the last two decades is unlikely to fully elucidate processes controlling long-term centennial to millennial-scale ice-stream behavior. Furthermore, there are relatively few state-of-the-art numerical ice-stream models which can track grounding-line movement [Pattyn and Payne, 2006; Pattyn *et al.*, 2012] and they have rarely been applied to real-world examples of past ice flow and lack validation at century to millennial time-scales. Nevertheless, quantifying the controls upon the transient behavior of an ice stream over these longer periods is crucial in order to reduce the uncertainties in predictions of future ice sheet stability.

[6] Here we focus on understanding forcing mechanisms and controlling factors on centennial to millennial-scale ice stream retreat. Importantly, the paleo record provides a means through which we can investigate temporal and spatial patterns of ice-stream retreat following the last deglaciation. One of the most detailed existing records of paleo-ice-stream retreat is that derived from recent high-resolution marine geophysical investigations of the former Marguerite Bay Ice

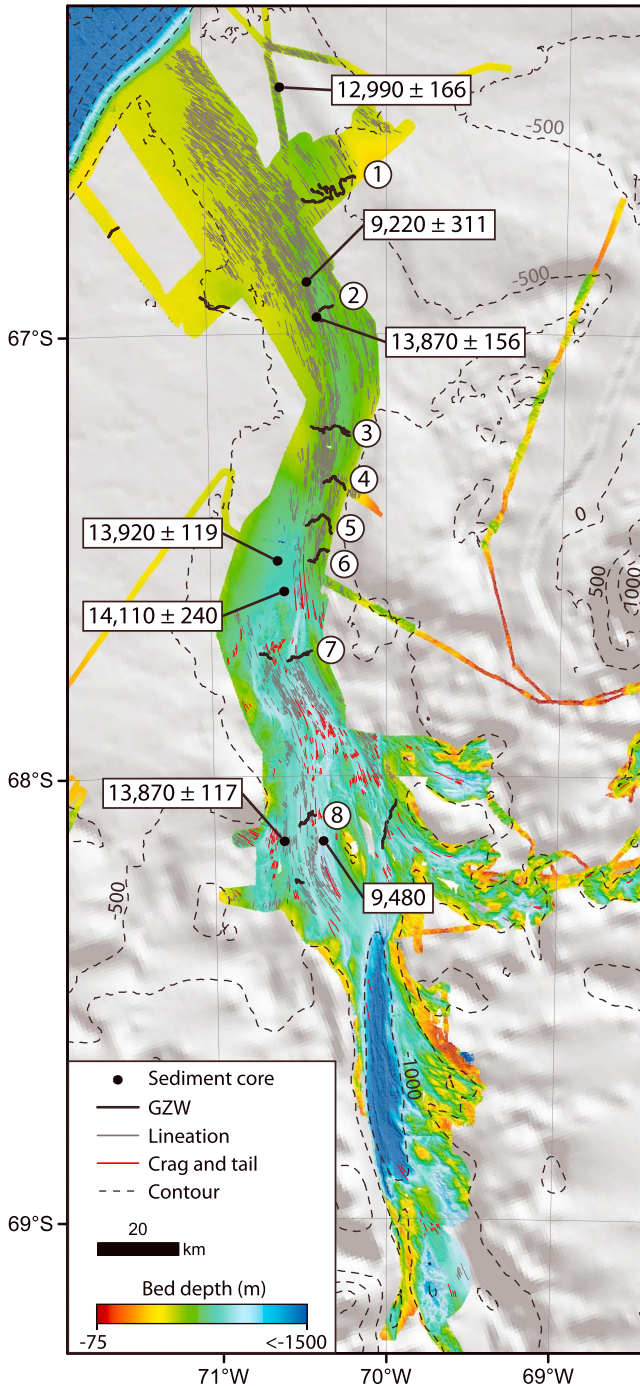


Figure 2. Marine geophysical landform assemblage of Marguerite Bay paleo-ice stream. Ice flowed from south to north (bottom to top). Boxes showing minimum deglacial ages in cal yr B.P. (\pm error where available) are from sediment cores (black dots) in Marguerite Trough [Pope and Anderson, 1992; Heroy and Anderson, 2007; Kilfeather et al., 2011]. Grounding-zone wedges used to assess the model retreat behavior are numbered 1–8. Landform data are from Livingstone et al. [2013]. The base map shows the distribution and elevation of available multibeam data (colored) superimposed upon a hillshade of BEDMAP2 bed topography with 500 m contour intervals [Fretwell et al., 2013].

Stream in the western Antarctic Peninsula [Ó Cofaigh et al., 2005, 2008; Kilfeather et al., 2011; Livingstone et al., 2013]. Recent work indicates that localized ice-stream geometry was an important influence on MBIS grounding-line retreat rates [Jamieson et al., 2012]. Building on that work, we explore the sensitivity of MBIS retreat to external forcing processes and internal factors. To achieve this, we constrain a numerical model of ice-stream grounding-line dynamics using detailed landform maps derived from marine geophysical data and subject the model to a range of forcing mechanisms and patterns to drive retreat.

2. Study Area and Deglacial History

2.1. Setting and Evidence for a Paleo-Ice Stream

[7] Marguerite Bay is a large embayment off the coast of the western Antarctic Peninsula (AP) bisected by a south-north trending topographic trough extending approximately 370 km from the mouth of George VI Sound to the continental shelf break (Figure 1). Mega-scale glacial lineations (MSGs) observed on the floor of Marguerite Trough (Figure 2) indicate that an ice stream drained this section of the Antarctic Peninsula Ice Sheet during the Last Glacial Maximum (LGM) [Ó Cofaigh et al., 2002, 2005; Livingstone et al., 2013]. The landform orientations indicate that streaming occurred along the full length of the trough and continued during retreat [Ó Cofaigh et al., 2008]. The trough floor has a “reverse slope”, deepening inland from 500 m below present sea level at the continental shelf edge to 1500 m below sea level at its deepest point (Figure 2). The trough continues under the modern George VI ice shelf and, although it has only been mapped at low resolution in this area, it is thought to be up to 1000 m deep [Graham et al., 2011].

[8] A series of radiocarbon dates from marine sediment cores (Figure 2) constrain the timing of grounding-line retreat in Marguerite Bay. They show that the MBIS began to retreat from its maximum extent at the continental shelf break before $14,110 \pm 240$ cal yr. B.P. [Pope and Anderson, 1992; Kilfeather et al., 2011]. The grounding line retreated by approximately 140 km from the outer to the middle shelf within the error of the deglacial dates (Figure 2). This implies rapid retreat of the MBIS across the outer and middle shelf, an interpretation supported by the lack of major cross-cutting MSGs and only a thin or absent drape of deglacial sediments overlying subglacial till in cores from the outer shelf [Ó Cofaigh et al., 2005; Kilfeather et al., 2011]. There are, however, two caveats to this. First, in line with most marine radiocarbon dates on ice-sheet retreat from the Antarctic shelf, these dates are from above the till/glacimarine contact and are therefore minima on grounding-line retreat. Retreat could therefore have happened earlier. Second, based on the range in the calibrated dates (Figure 2), the maximum length of time for retreat would have been 636 years.

[9] A series of 10 large sedimentary wedges in Marguerite Bay (Figure 2) are interpreted as grounding-zone wedges (GZWs) [Livingstone et al., 2013]. They range from 10 to 30 m thick at their downstream end and are between 5.8 and 14 km long. Eight of these are located within the zone of ice streaming, and all have MSGs superimposed on their upper surface. GZWs are thought to form at the ice-stream grounding line when there has been sufficient time for sediment to accumulate [Powell and Domack, 1995; Dowdeswell et al., 2008;

Dowdeswell and Fugelli, 2012] and thereby indicate positions where the grounding line is relatively stable or even slowly advancing. We note that four closely spaced GZWs (numbers 3–6; Figure 2) on the outer shelf are located where rapid, potentially unstable, ice-stream retreat might otherwise be predicted as a result of the steep reverse-sloping ice-stream bed [Weertman, 1974; Thomas and Bentley, 1978; Schoof, 2007; Jamieson et al., 2012].

2.2. Hypothesized Controls on the Retreat of the MBIS

[10] Based on observations from the paleo record, a number of forcings and factors are hypothesized to have controlled the retreat of MBIS. The onset of retreat, before 14.1 ka B.P. [Pope and Anderson, 1992], broadly coincides with meltwater pulse 1a [Fairbanks, 1989], and it has therefore been suggested that sea-level rise triggered its initial retreat [Kilfeather et al., 2011]. Because of the reverse-sloping bed, rapid grounding-line retreat could be expected across the outer trough, and sedimentological analyses suggest an ice shelf was present during this initial phase of retreat [Kilfeather et al., 2011]. Once the grounding line had reached the inner shelf, the calving front then retreated gradually from the middle shelf between approximately 13.2 and 12.5 ka B.P., indicating that the ice shelf reduced in size, therefore reducing its buttressing effect.

[11] Down core changes in benthic foraminiferal assemblages indicate that during the gradual retreat of the calving front, a warm water current may have flowed into Marguerite Trough, presumably enhancing melting beneath the ice shelf [Kilfeather et al., 2011]. Another phase of warm water incursion, from Circumpolar Deep Water, coincides with the cessation of calving into the embayment, suggesting that much of the ice shelf had been removed, reducing buttressing conditions at the terminus [Kilfeather et al., 2011]. Thus, any combination of rising sea level, enhanced ocean-driven melt, or reduced ice-shelf buttressing may have allowed ice discharge and ice-stream thinning to accelerate, resulting in grounding-line retreat via flotation. In addition, recent numerical modeling suggests that aside from the basal topography, the width of the MBIS channel strongly controlled grounding-line retreat rates [Jamieson et al., 2012]. However, although the broad data-model fit was good, the model did not include an ice shelf and did not systematically investigate the sensitivity of the ice stream to different external forcing processes, which is what we investigate in this paper.

3. Modeling Approach

3.1. Outline

[12] We combine a simple one-dimensional flowline model that includes a dynamic and robust representation of grounding-line behavior [Vieli and Payne, 2005; Jamieson et al., 2012; Pattyn et al., 2012] with the marine geophysical record of MBIS flow and retreat on the continental shelf [Livingstone et al., 2013]. The GZW locations permit an independent assessment of the model’s ability to reproduce the episodic pattern of retreat. We explore the sensitivity of the model to a range of forcing mechanisms in order to determine the governing controls of grounding-line retreat. In doing so, we carry out one of the first millennial-scale, fully dynamic modeling assessments of paleo-grounding-line behavior. Our approach consists of three main steps: (i) the buildup of an

initial LGM condition for the model, (ii) an exploration of the response and sensitivity of the ice stream to various simple forcings (climate, ocean, sea level, and ice-shelf buttressing), and (iii) a further exploration of retreat sensitivity to local topographic controls.

3.2. Numerical Model of Ice Stream and Grounding-Line Evolution

[13] The simulation of dynamic grounding-line evolution and response is not well-suited to low-resolution fixed-grid models that are commonly used to simulate long-term ice-sheet evolution [Vieli and Payne, 2005; Pattyn et al., 2012]. We therefore use a one-dimensional numerical flowline model that is specifically designed for tracking grounding-line motion [Vieli and Payne, 2005; Nick et al., 2009; Jamieson et al., 2012] and extend it to include a buttressing ice shelf and sub-ice shelf oceanic melting.

[14] The time-dependent evolution of ice flow, ice surface, and internal stress is calculated along an 800 km flowline derived by tracing lineated landforms in Marguerite Bay (Figure 1). Using a width- and depth-averaged formulation of the stress balance, driving stress τ_d is balanced by basal and lateral shear stress (τ_b and τ_{lat} , consecutively) and longitudinal stress gradients ($\partial\tau_{xx}/\partial x$), in the direction of ice flow x :

$$\frac{\partial\tau_{xx}}{\partial x} + \tau_b + \tau_{lat} = \tau_d \quad (1)$$

[15] We follow the widely used approach of *van der Veen and Whillans* [1996] for calculating lateral drag which assumes zero flow at the ice stream margins. As a basal boundary condition, we use a Weertman-type nonlinear sliding relation [Weertman, 1957] that is a function of effective pressure, N , at the bed. For an ice stream of thickness H and half width W , the stress balance (equation (1)) results in an expression for depth- and width-averaged ice flow u given by

$$2 \frac{\partial}{\partial x} \left(H v \frac{\partial u}{\partial x} \right) - \beta \left(\frac{u}{N} \right)^{1/m} + \frac{H}{W} \left(\frac{5u}{2AWf_{lat}} \right)^{1/n} = \rho_i g H \frac{\partial S}{\partial x} \quad (2)$$

where the constants ρ_i and g are the density of ice (910 kg m⁻³) and gravitational acceleration, respectively, S is the ice surface, A is the flow rate factor [Glen, 1955], β is the basal sliding coefficient referring to a Weertman-type sliding relation [Weertman, 1957], n and m are the exponents for ice flow and sliding relations, respectively, (both taken as 3), and f_{lat} is a buttressing factor (described below). Equation (2) is solved by iterating for the effective viscosity v , given by

$$v = A^{-1/n} \left| \frac{\partial u}{\partial x} \right|^{(1-n)/n} \quad (3)$$

[16] Ice surface evolution explicitly accounts for the along-flow variation in ice-stream width and surface accumulation, a , using

$$\frac{\partial H}{\partial t} = a - \frac{1}{W} \frac{\partial(uHW)}{\partial x} \quad (4)$$

[17] In the recent Marine Ice Sheet Intercomparison tests [Pattyn et al., 2012], the model was found to have a robust treatment of grounding-line motion that is consistent with

a boundary layer theory [Schoof, 2007], which is important to avoid issues imposed by model numerics [Vieli and Payne, 2005].

[18] Conditions at the grounding line are determined as follows:

[19] 1. A flotation criterion is applied to calculate the location of the grounding line for the evolving ice thickness at each time step.

[20] 2. The grounding line is tracked continuously and accurately using a moving grid, which avoids grid-size dependency typically found in fixed-resolution models [Vieli and Payne, 2005; Pattyn et al., 2012]. Initial grid resolution is approximately 900 m and reduces to a minimum of approximately 100 m as the grounding line retreats to the head of George VI Sound.

[21] 3. The model in this study differs to earlier versions [Vieli and Payne, 2005; Jamieson et al., 2012] in that a 20 cell length (approximately 18 km long at maximum MBIS extent) and laterally-confined ice shelf is added downstream of the grounding line, which buttresses the upstream ice via lateral stress transmission to the ice-stream sides [Dupont and Alley, 2005]. Following the moving grid framework of the model, the initial ice-shelf cell resolution is approximately 900 m and changes as the position of the grounding line is recalculated. Any remaining ice is immediately calved beyond the front of the ice shelf. A buttressing factor, f_{lat} (equation (2)), controls the strength of the transmission of lateral drag to the sides where a default value of $f_{\text{lat}}=1$ applies the full effect of buttressing from the ice shelf, with values of $f_{\text{lat}} > 1$ nonlinearly reducing the resistive effect of the buttressing.

[22] 4. Beneath the ice shelf, ocean melt rates, M , are applied using a parameterization that depends linearly on water depth. From a minimum rate of 0.1 m yr^{-1} at the ocean surface, ocean melt increases to a maximum value, M_{max} , at a depth of 500 m, below which it is constant ($M=M_{\text{max}}$).

[23] 5. The longitudinal stress at the ocean boundary is balanced by the difference in hydrostatic pressure between the ice front and the ocean water [Vieli and Payne, 2005]. This stress balance results in a boundary condition for the velocity gradient at the ice-stream front given by

$$\left. \frac{\partial u}{\partial x} \right|_{\text{Front}} = A \left[\frac{\rho_i g}{4} \left(1 - \frac{\rho_i}{\rho_w} \right) \right]^n H^n \quad (5)$$

where the density of the ocean water, ρ_w , is set to 1028 kg m^{-3} . Surface accumulation (a), sea level, rate factor (A ; corresponding to ice temperature), ocean melt (M_{max}), and ice-shelf buttressing factor (f_{lat}) are time dependent to enable sensitivity testing.

3.3. Boundary Conditions and Geophysical Constraints

[25] The bed topography consists of high-resolution swath-bathymetric data that extend from the outer to inner trough, merged with a 1 km elevation data set covering the remainder of the Marguerite Bay area, including beneath the modern George VI Ice Shelf [Graham et al., 2011]. The high-resolution data underpin BEDMAP2 [Fretwell et al., 2013] in this region, but we remove the topographic expression of each GZW to approximate topography prior to their deposition. For the minimal upstream part of the ice stream that lies above sea level, elevation is prescribed by ALBMAP v1 [Le Brocq et al., 2010], which is based upon BEDMAP [Lythe et al., 2001] in

Table 1. Sensitivity Experiment Set Details^a

Set	Set Description	Topography Depth	Topography Width	Sea-Level Forcing (m)		M_{max} Forcing (m yr^{-1})		f_{lat} Forcing		Ice Temperature Forcing		# of expts. Linear	Step
				Linear (Increase per kyr From -100m)	Step (Increase per kyr From -100m)	Linear (Increase per kyr From 10m yr^{-1})	Step (Increase per kyr)	Linear (Increase per kyr From 1)	Step	Linear (Increase per kyr From -24°C)	Step		
1	Sensitivity to geometry	Normal, flat, tilt	Normal, +10%, +20%, straight	Fixed at -100	-	20	-	Fixed at 1	-	Fixed at -24	-	6	0
2	Sensitivity to single forcing	Normal	Normal	0, 2, 5, 10, 20, 30, 40, 60, 100	10, 20, 40, 60, 100	0, 5, 10, 20, 30, 40	5-10, 5-20, 5-40	0, 0.1, 0.5, 1, 5, 10, 100, 1000, 5000	10,000	0, 0.5, 1, 2, 3	2, 5	26	11
3	Sensitivity to multiple forcings	Normal	Normal	0, 2, 5, 10	-	0, 2, 5, 10	-	0, 0.1, 0.5, 1, 5, 10, 100, 1000	-	0, 0.5, 1, 2, 3	-	112	0
4	Sensitivity to fluctuating forcings	Normal	Normal	0, linear 20 m, modeled	-	20	-	0, 10	-	EPICA scaled	-	5	-

^aChanges to topography (set 1; Figure 3) and rates of change of forcing factors (sets 2-4; Figure 4) are outlined alongside the number of experiments in each set. A “-” indicates that a particular forcing pattern is not applied within an experiment set.

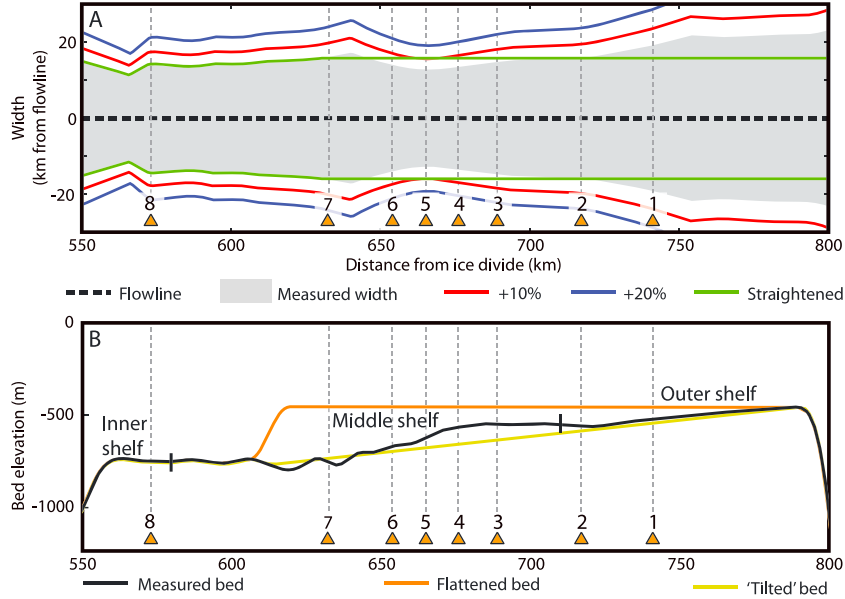


Figure 3. Along-flow geometric boundary conditions in the outer to middle shelf area for sensitivity Experiment Set 1. (a) Lateral geometry modifications (colored lines) compared to the mapped width (grey shading). (b) Bed geometry modifications (colored lines) compared to mapped bed depth (black line). Grounding-zone wedges (orange triangles and grey dashed lines) are numbered 1–8 as in Figure 2. Divisions between outer, middle, and inner continental shelf are shown by black crosshairs.

this area and is not significantly different from BEDMAP2 [Fretwell *et al.*, 2013].

[26] Orientations of MSGLs define the central model flow line and the model width is defined by the lateral distribution of MSGL where available. The lateral extents of the MSGL often correspond to a topographic break in slope, which represents the shoulder of the trough. Therefore, where the swath-bathymetric data are laterally limited, we assume that most of the ice-stream flow took place within the bounds of the trough shoulders, using them to define the ice-stream width (Figures 1 and 2). The width ranges from 45 km at the shelf edge to 25 km in the region of steepest reverse slope. Beyond the continental shelf break, we rapidly increase the width to simulate a laterally unconfined system. The flowline extends to the modern ice divide, and in this inland region, the ice-stream width is determined by the topographic ridgeline.

[27] Sedimentological analyses of the upper till indicate that basal shear stresses of 10–30 kPa would have been supported during retreat [Ó Cofaigh *et al.*, 2005; Kilfeather *et al.*, 2011] and these values are used as a constraint for the basal sliding parameter β . In the model, an initial basal slip mask (β_{mask}) has low initial values to represent reduced friction areas below sea level and higher values to represent an assumed stiffer bed above sea level. This is modified as a function of effective pressure to calculate β at each time step:

$$\beta_{\text{below sea level}} = \frac{\beta_{\text{mask}}(\rho_i H + \rho_w z)}{5e^5} \quad (6)$$

and

$$\beta_{\text{above sea level}} = \frac{\beta_{\text{mask}} \rho_i H}{5e^5} \quad (7)$$

where z is bed elevation and is negative below sea level. The less slippery nature of minor bedrock outcrops on the trough

floor of the outer and middle shelf [Pope and Anderson, 1992; Ó Cofaigh *et al.*, 2002] is not incorporated into the slip condition because they do not extend across the entire trough width.

[28] Accumulation follows the modern day spatial pattern [Arthern *et al.*, 2006] but is reduced by 60% to account for drier LGM conditions [e.g., Siegert and Payne, 2004; Wolff *et al.*, 2010] while also enabling the grounding line of the initial ice stream to stabilize at the continental shelf edge. No melt is prescribed at the ice surface.

3.4. Experimental Design

[29] Four sets of experiments (totaling 160 individual sensitivity experiments) are carried out (Table 1). First, to understand the sensitivity of the ice stream and, more specifically, grounding-line retreat rate to local topographic variations, we systematically modify the bed geometry (by flattening or tilting the outer trough) and ice-stream width (by straightening or widening the outer trough) (Figure 3) and note differences in retreat responses. Second, we investigate the dynamic response to simple time-dependent external forcing factors (Figure 4). Retreat responses to multiple forcing factors and fluctuating forcing factors (Figure 4) make up the third and fourth sets of experiments, respectively.

[30] These experiment sets are all initiated from a stable (steady state) “LGM” ice-stream configuration in order to avoid initial adjustment effects that are unrelated to effects from imposed perturbations. To generate the initial steady state model, the maximum rate of melting under the ice shelf (M_{max}) is held constant at -20 m yr^{-1} and the full resistive potential of the ice shelf is felt ($f_{\text{lat}} = 1$). Sea level is held static at 100 m below present-day levels, and the model is run until the ice surface stops evolving. To drive the ice-stream retreat experiments, time-dependent variations in relative sea level, air temperature (applied instantaneously to the ice temperature

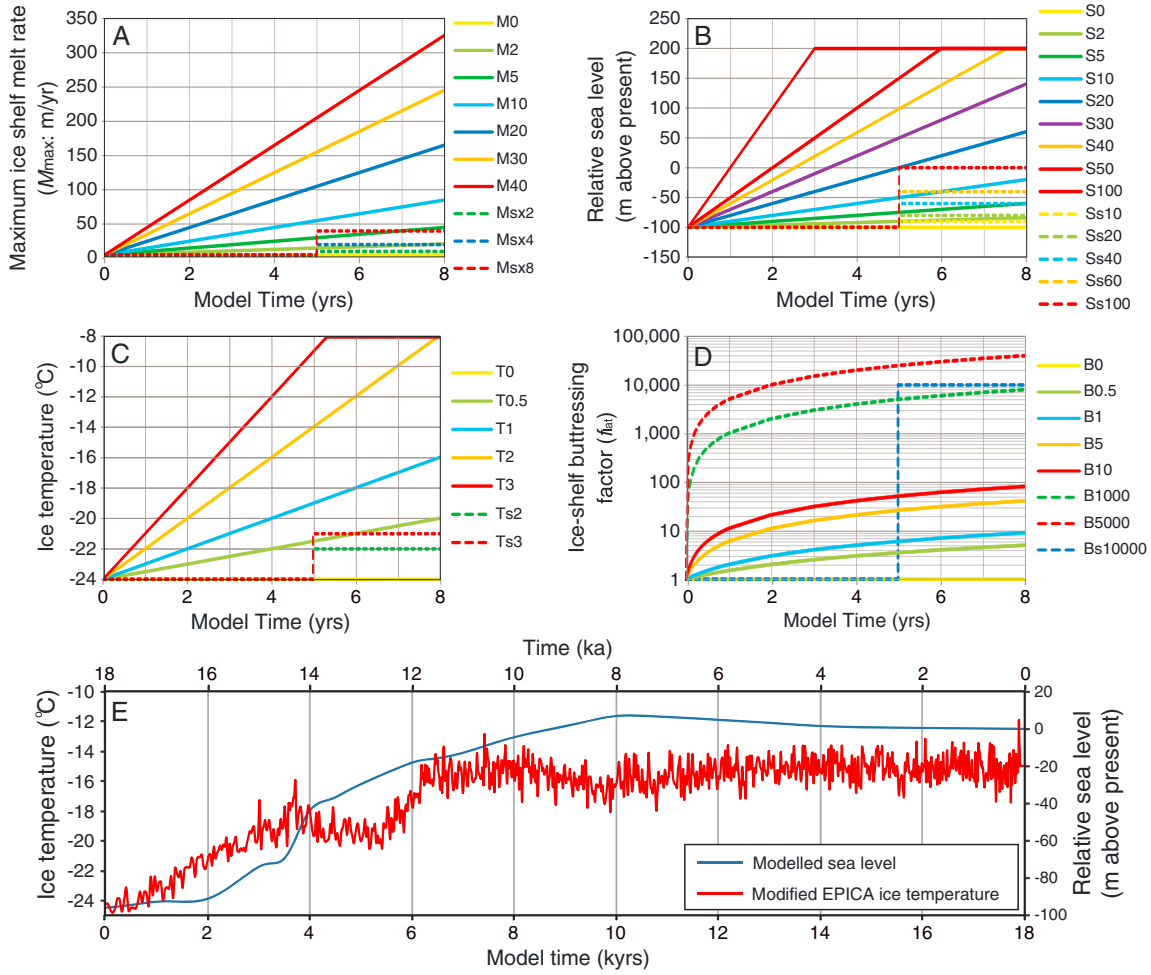


Figure 4. Forcings applied during ice stream retreat sensitivity experiments after an initial 2 kyr period of static forcing. Panel legend labels correspond to naming convention for experiments. Note that for (a) maximum ice shelf melt rate, time-dependent forcing starts at 5 m yr^{-1} . (b) Sea level is not forced beyond 200 m above modern and (c) increases in ice temperature are limited once a value of -8°C is reached. (e) The nonlinear forcings through time (ka) and model time (kyr) based on locally modeled sea level change [extracted from *Peltier, 2004*] and rescaled and shifted EDC ice temperature fluctuations [*Masson-Delmotte et al., 2010*].

via rate factor A), maximum ocean-driven melt (M_{max}), and ice-shelf buttressing factor (f_{lat}) are applied (Figure 4).

[31] In the first three sets of experiments, forcings are applied either linearly or in a step, in order to understand grounding-line sensitivity to different magnitudes of gradual change or to rapid events. Realistic magnitudes and rates of change since the LGM are difficult to define from the paleo record but modeling and observations of modern rates help indicate potentially realistic upper limits. For example, since the LGM, sea level may have risen by approximately 100 m at up to approximately 20 m kyr^{-1} (Figure 4e) [*Peltier, 2004*] and ice temperature could have warmed by up to 12°C at rates of up to 6°C kyr^{-1} (Figure 4e). Modern ocean-driven melt rates are $3\text{--}5 \text{ m yr}^{-1}$ under the George VI shelf [*Jenkins and Jacobs, 2008*] but may have been larger under the thicker ice in the past due to melt by warm water plumes at depth, as is identified in the region today [*Smith et al., 1999; Holland et al., 2010*]. The maximum modern rate of melting under the Pine Island Glacier (PIG) is up to 40 m yr^{-1} [*Rignot and Jacobs, 2002; Jacobs et al., 2011*] and indicates a plausible

maximum. A range of forcing rates, chosen to explore ice-stream sensitivity beyond these limits, is applied to the model (Table 1) over a period of 8 kyr.

[32] In the fourth experiment set, nonlinear forcings are applied for ice temperature and sea level based upon available paleo records. Four experiments are forced by ice temperature fluctuation patterns from the European Project for Ice Coring in Antarctica (EPICA) Dome C (EDC) ice core record [*Masson-Delmotte et al., 2010*]. The purpose of using this record is to explore the effect on retreat by episodic, short-term variations in temperature forcing overprinted on long-term climatic trends. The record is scaled and shifted to account for the low elevation of the ice stream in comparison to the EDC site, resulting in values of between -24.25°C at 18 ka and -15°C at present day (Figure 4e). The section of the record between 18 ka and 10 ka is used in these sensitivity experiments and has a resolution of 16–47 years during this period [*Jouzel et al., 2007*]. Another 17 experiments apply linear temperature and ice-shelf melt forcings alongside a local sea-level history (Figure 4e) extracted from the ICE-5G model

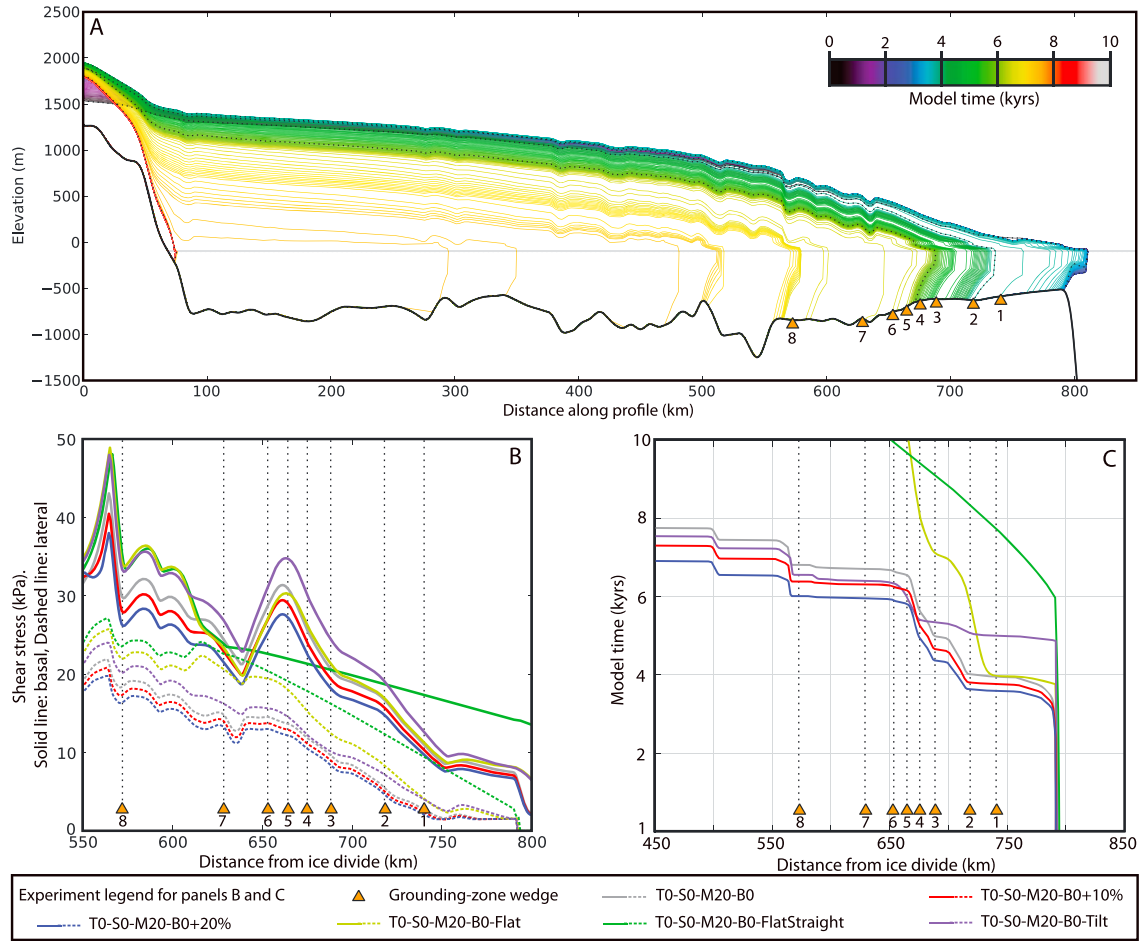


Figure 5. Model sensitivities to bed and width geometry. (a) Modeled along-flow ice-surface and grounding-line evolution every 250 years (colored lines) and every 2 kyr (dashed black lines) along the MBIS basal topography (solid black line) for the non-geometrically modified benchmark model (*T0-S0-M20-B0*). As the grounding-line position slows down (higher density of colored lines intersecting the bed), thinning in the upstream area continues. (b) Shear stresses in each of the geometric sensitivity tests (experiment legend identifies individual models as in supporting information Table S1). In all but model *T0-S0-M20-B0-FlatStraight*, lateral shear stress peaks between GZWs 3 and 6. (c) Grounding-line position over time. In the normal, 10% and 20% increased width models the grounding line retreats in a stepped (rapid/slow/rapid) nature, slowing near GZWs. Stepped retreat patterns in the flattened and tilted bed experiments are less well defined. In the flattened and straightened bed experiment, there is very little variation in retreat rate. Output in Figures 5a and 5c include the 2 kyr model initialization prior to the introduction of time-dependent forcing.

[Peltier, 2004]. The aim is not to reconstruct a precise retreat pattern but to identify how nonlinear records of approximately realistic shape may impact upon retreat behavior.

[33] Experiments are labeled with the following convention, where x denotes the rate of change per kyr: Sea-level forcing (Sx); Ice-temperature forcing (Tx); Maximum sub-ice-shelf melting— M_{\max} (Mx); Buttressing factor— f_{lat} (Bx). The subscripts s or m next to the forcing label indicate that the forcing is either stepped or derived from model output, respectively, as opposed to the default of a linear increase. For example, hypothetical experiment $Ts_2-S10-Ms_2-B0$ would be forced by a 2°C step in ice temperature, a linear 10 m kyr⁻¹ increase in sea level, a 2 times step in melt rate such that M_{\max} steps from the initial rate of 10 m yr⁻¹ to a rate of 20 m yr⁻¹, and an ice-shelf buttressing factor that is unchanged from the initial value (see tables in the supporting information).

4. Results

4.1. Set 1: Sensitivity to Bed Topography and Ice-Stream Width

[34] The pattern of retreat in a non-topographically perturbed experiment forced by linearly increasing ice-shelf melt rate is highly nonlinear and steplike (Figures 5a and 5c; model *T0-S0-M20-B0*) and acts as a control for comparing retreat-rate sensitivity against adjusted geometry experiments. Results show that nonlinear retreat rates are observed in all geometry-based sensitivity tests unless the width and bed are both straightened over the outer trough, in which case the retreat rate becomes nearly linear (Figure 5c; model *T0-S0-M20-B0-FlatStraight*). For the nonlinearly responding experiments, retreat slows where the grounding line moves into locations where the trough narrows or where basal topographic

features present pinning points. During these slowdowns in retreat, the ice stream continues to lose mass via upstream thinning (Figure 5).

[35] Such nonlinearity occurs even when the bed is flattened while retaining the known trough width (Models *T0-S0-M20-B0-Flat*). Analysis of the basal and lateral stress regimes in the model indicates that beside the importance of bed topography, width-controlled lateral drag is a key control on the pattern of faster versus slower grounding-line retreat. Compared to the straight width case (*T0-S0-M20-B0-FlatStraight*), lateral drag is enhanced by between 20 and 30% in the narrowest portion of the ice stream where GZWs 3–6 are found, while basal shear stress remains consistently low (Figure 5b). Slowdowns in retreat rate are observed in the narrowest portion of the trough, even when the bed slope is in an exaggerated reverse-sloped configuration (*T0-S0-M20-B0-Tilt*) generated using a linear interpolation between the shelf edge and the base of the known reverse slope resulting in a reverse bed slope with an angle of 0.115° (Figure 3).

[36] Our experiments also indicate that any uncertainty related to our delineation of the trough width using the bathymetric expression of its margin, which is a gradual rather than sharp break (Figure 2), does not significantly influence retreat patterns. For example, by adding 10 or 20% to the model width (Figures 3 and 5; *T0-S0-M20-B0 + 10% or +20%*), retreat patterns remain consistent with the non-topographically modified experiment, but the rates of retreat are 15 or 30% faster, respectively, across the region containing the GZWs. It is likely, however, that non-uniform modifications to the trough width may alter the retreat patterns slightly. In combination with previous work [Jamieson et al., 2012], the set 1 results demonstrate that the pattern and speed of grounding-line retreat are controlled not only by basal topography but are also highly sensitive to along-flow variability in the trough width either with or without an ice shelf.

4.2. Set 2: Dynamic Retreat Response to Single Linear Forcings

[37] The response of the grounding-line position to the imposition of linear changes with time in either ice temperature, sea level, ocean-driven melting, or ice-shelf buttressing is shown in Figure 6. Not all forcings result in an onset of retreat from the continental shelf break (supporting information Table S1). Where a retreat response is modeled, the timings of the onset of retreat from the continental shelf break are highly variable, and the only experiments to show a grounding line that fully retreats along the entire Marguerite and George VI troughs are those forced by enhanced ocean-driven melting or ice temperature increases that are beyond likely changes since the LGM (supporting information Table S1). In six of the single forcing experiments the grounding line retreats past all eight GZWs in Marguerite Trough, with another four displaying partial retreat (Figure 6). All of these experiments display a highly nonlinear response despite the linear forcing. The locations of slowdowns in retreat rate are spatially consistent and occur in close proximity to mapped GZWs (Figure 6). Notably, major retreat slowdowns occur in the area between GZWs 3–6, where the reverse bed slope is steepest. Between GZWs 4 and 5, slowdowns in retreat last approximately 200–2500 years depending on the magnitude of forcing (Figure 6). Unsurprisingly, the initial timing and general rate of grounding-line retreat are controlled by

the magnitude and rate of forcing enhancement (supporting information Table S1).

[38] Experiments suggest that grounding-line retreat is relatively insensitive to changes in A (ice temperature), which is being used to investigate the influence of air temperature upon retreat. Indeed, retreat is not initiated by temperature forcing unless unrealistically high warming is prescribed (supporting information Table S1 and Figure 6a). Retreat only occurs in the two experiments (*T2-S0-M0-B0* and *T3-S0-M0-B0*), where the ice has warmed to above -9°C , a value above the mean annual air temperature threshold for the stability of ice shelves in the modern Antarctic Peninsula [Cook and Vaughan, 2010]. The warm ice temperature increases the ice softness, and consequently the ice flux, enough to thin the terminus below flotation. When retreat is driven by rapid temperature rises (e.g., by 3°C kyr^{-1} ; *T3-S0-M0-B0*), the grounding line takes just over 1 kyr to pass over the locations of the GZWs (Figure 2 and supporting information Table S1). Retreat in this experiment is around 50% faster across the core sites than any of the other singly forced simulations, the quickest of which is approximately 2.1 kyr in the case of the most rapid sub-ice-shelf melt rate acceleration experiment (*T0-S0-M40-B0*; supporting information Table S1).

[39] Sea-level rise initiates retreat from the continental shelf edge only in unrealistic scenarios. For example, retreat begins when a high rate of $>20\text{ m kyr}^{-1}$ is sustained over at least 5.5 kyr (Figure 6b) and sea level crosses a threshold between 35 and 46 m above present (supporting information Table S1). However, even the regional Holocene sea level highstand was only 14.5 to 16 m above modern [Bentley et al., 2005]. Regardless of this, once retreat is initiated, it remains relatively slow and does not pass all of the GZWs or core sites within the modeled time period (Figure 6b and supporting information Table S1), suggesting that sea-level rise is not solely responsible for driving retreat.

[40] The sensitivity of retreat to enhancement of melting beneath the ice shelf (M_{max}) is stronger than to other forcing factors, although this sensitivity reduces with more rapid increases in M_{max} (Figure 6c). Regardless of the rate at which M_{max} is increased, retreat consistently begins when M_{max} reaches a threshold of between 31 and 33 m yr^{-1} (supporting information Table S1), a value consistent with that experienced under the modern IIG [Jacobs et al., 2011]. Not all M_{max} forced experiments retreat fully over the Marguerite Trough GZWs. Those that do (*T0-S0-M20-B0*, *T0-S0-M30-B0*, *T0-S0-M40-B0*) take between 1.8 and 2.8 kyr with retreat timing being inversely related to the rate at which M_{max} is increased. Despite the sensitivity of retreat to changes in melt rate, these timescales are considerably longer than the retreat chronology reconstructed from the radiocarbon-dated sediment cores along the trough.

[41] As a sole forcing, gradual ice-shelf debuttressing is ineffective in driving retreat and results in no significant movement of the grounding line (supporting information Table S1 and Figure 6d). This is unsurprising because for the initial geometry, the ice shelf extends beyond the continental shelf and becomes laterally unconfined, thus minimizing the buttressing effect at the LGM. In the most rapid debuttressing experiment, ice velocities at and behind the terminus increase by only around 5% which is not enough to destabilize the MBIS grounding line over the simulation period.

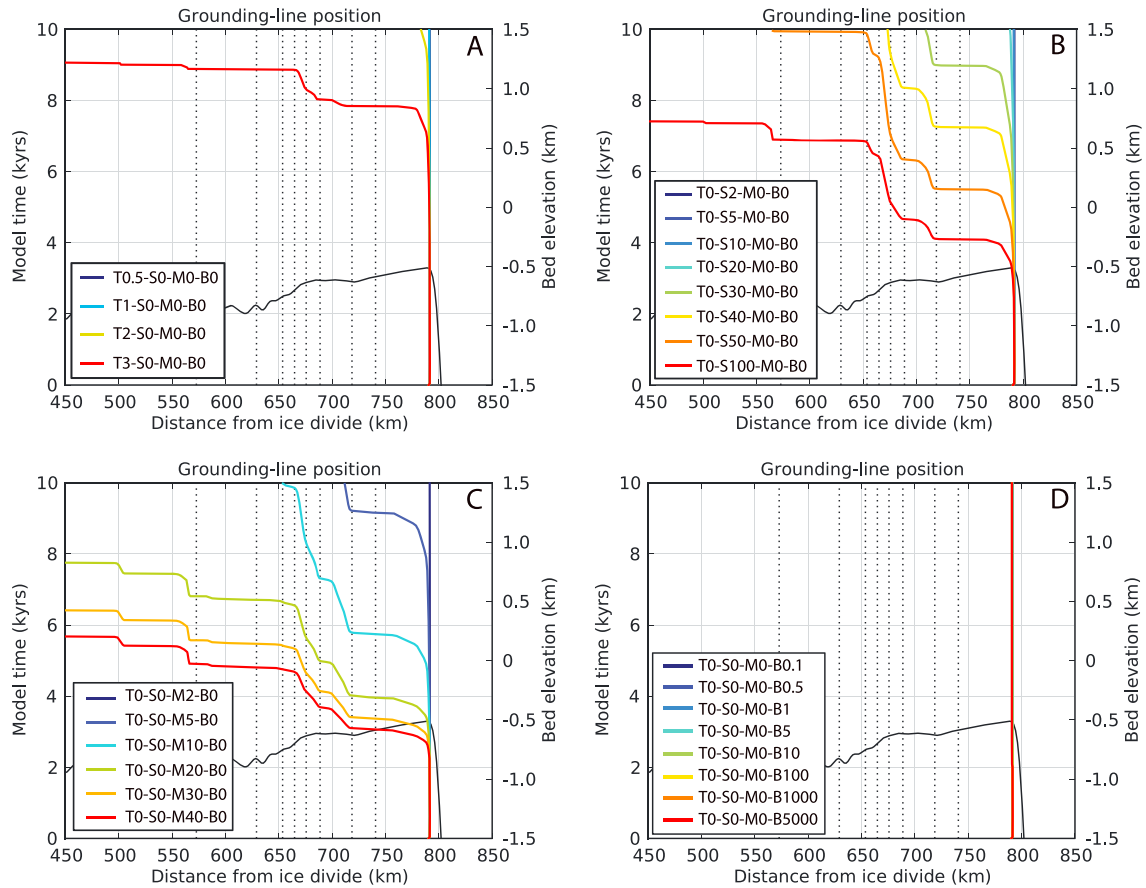


Figure 6. Modeled grounding-line positions as single-forced experiments retreat across the outer shelf of Marguerite Trough through model time. Note that where retreat is induced, it is punctuated and nonlinear despite the linear forcing. (a) Ice-temperature forcing: only model *T3-S0-M0-B0* retreats past the GZWs. (b) Sea-level forcing: accelerated sea-level rise speeds up retreat and allows earlier retreat onset. However, retreat past the GZWs always takes 2.8 kyr or longer. (c) Sub-ice-shelf melt forcing: shows that retreat rates increase with enhanced melt rates but that this sensitivity reduces as melt rates increase. (d) Ice-shelf debuttressing forcing: indicates that the removal of an ice shelf in gradual or abrupt manner does not cause retreat onset, with all models showing no response. For individual experiment result details, see supporting information Table S1. The solid black line is the bed elevation, and the dashed vertical lines show the locations of GZWs (Figure 2).

[42] The above experiments are consistent with retreat from the continental shelf beginning once a critical threshold in forcing is reached. However, the linear forcing experiments described above assume that any forcing changes were gradual. The introduction of a stepped increase in either ice temperature (by 2°C or 5°C), sea level (by 10, 20, 40, 60, or 100 m), M_{\max} (by 2, 4, or 8 times), or an instantaneous and complete loss of ice-shelf buttressing induce limited response from the MBIS (supporting information Table S1). Where a retreat response is observed ($8\times$ increase in M_{\max} or 100 m sea-level rise), the grounding line retreats immediately and stabilizes inland of the deepest part of the outer continental shelf, where the bed slope begins to shallow. Where grounding-line retreat is not initiated, ice-surface thinning since the beginning of the “event” still occurs. For example, at 200 km from the ice divide, thinning ranges from approximately 20 to 200 m under a 10 m rise in sea level or 5°C increase in ice temperature, respectively. In contrast, inland thinning is much more substantial (up to 350 m) when a retreat response at the grounding line occurs.

4.3. Set 3: Dynamic Retreat Response to Multiple Linear Forcings

[43] Retreat is more readily induced and accelerated by combining multiple forcings within a single simulation. We performed a total of 112 experiments in which two to three linear forcings from ice temperature, sea level, ocean-driven melting, and ice-shelf buttressing were combined (Figure 7 and supporting information Table S2). Although full retreat along George VI Sound does not occur in all experiments, where retreat across the continental shelf occurs, the spatial pattern of slowdowns and speedups in retreat rate are consistent with each other and with the single-forced experiments. Again, the most significant slowdowns occur between GZWs 4 and 5 where, depending on the strength of the forcing, the grounding line takes between approximately 250 and 3000 years to cover the approximately 10 km distance, which corresponds to an average retreat rate of 5–40 m yr⁻¹.

[44] The MBIS grounding-line retreat is most sensitive to combinations of either sea-level rise and ocean-driven melting or ice-temperature increase and ocean-driven melting

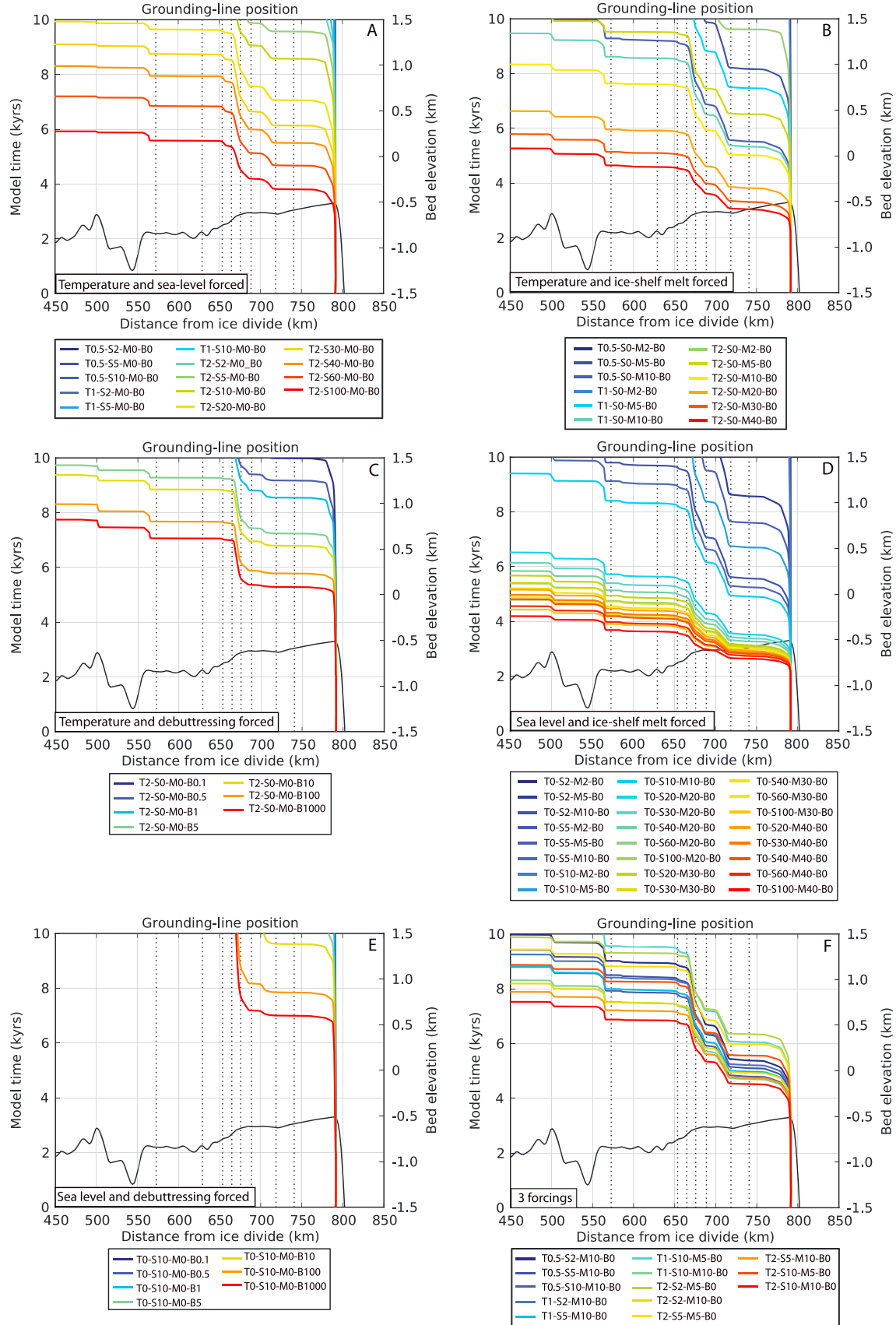


Figure 7

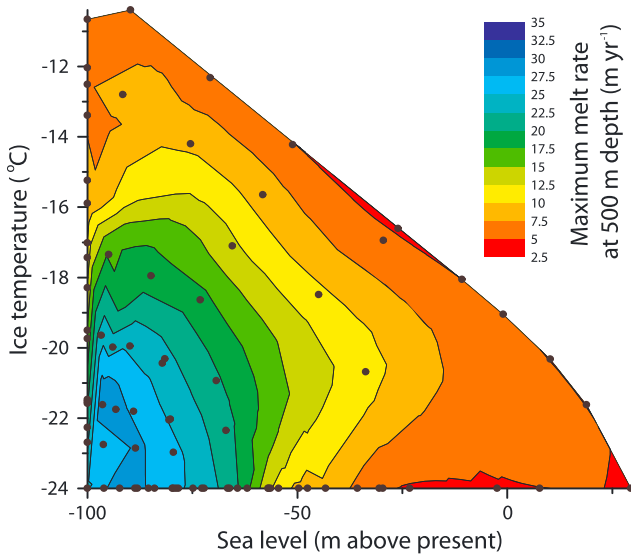


Figure 8. Ice temperature, sea level, and sub-ice-shelf melt rate forcing values reached at the time of initial retreat, indicating the interplay between forcing factors and their potential to initiate retreat of the MBIS. The data points (black dots) are linearly interpolated to identify likely values where sensitivity tests were not carried out. Note that by combining forcings, plausible external changes following “LGM” conditions (SL = -100 m, Ice temperature = -24°C , $M_{\text{max}} = 5 \text{ m yr}^{-1}$) can induce grounding-line retreat. For example, if a 20 m sea-level rise occurred in tandem with a 3°C ice temperature increase then retreat could be generated when sub-ice-shelf melting exceeded approximately 20 m yr^{-1} at 500 m depth. Alternatively, if there was 60 m of sea-level rise and ocean-driven melt rates reached 10 m yr^{-1} , then only approximately 2°C of ice warming would be required to initiate MBIS retreat.

(Figures 7b and 7d and supporting information Table S2). The combination of ocean-driven melting and sea-rise can be effective in inducing rapid retreat over the GZWs, taking as little as 1.05 kyr (supporting information Table S2) but only when forced by unrealistically high rates. We find that only two of the fully retreating models (T2-S0-M5-B0 and T0-S10-M5-B0) are forced at magnitudes that may have been realistic since the LGM. For example, by the time it has retreated past the GZWs, experiment T2-S0-M5-B0 reaches a sub-ice-shelf melt rate of 37.5 m yr^{-1} , a value consistent with the highest rate reported for modern Antarctica [Rignot and Jacobs, 2002; Jacobs et al., 2011] and has an ice temperature that has risen by 16°C , 25% higher than the LGM to Holocene rise recorded in the EDC ice core [Masson-Delmotte et al.,

2010]. We also note that extremely slow retreat, lasting up to 4.5 kyr, is possible via lower rates of these combined processes. For different sets of forcing, very similar patterns and rates of retreat are induced. Therefore, although forcing combinations which include both sea-level rise and increasing ocean-driven melting tend to cause faster retreat, the exact combinations of particular forcing regimes that controlled past grounding-line retreat cannot be distinguished clearly.

[45] The correspondence between the locations of retreat-rate slowdowns and the GZWs mapped on the floor of Marguerite Trough is strongest when buttressing from an ice shelf is simulated (Figures 7a, 7b, 7d, and 7f). This is shown in experiments combining warming ice temperature or rising sea level with debuttressing, where retreat is more linear and rapid between GZWs 2 and 3 (Figures 7c and 7e) in comparison to experiments that retain full ice-shelf buttressing effects (Figures 7a, 7b, and 7d). Furthermore, the inclusion of gradual debuttressing as a process alongside other forcing factors only makes small changes to the retreat timescale (supporting information Table S2).

[46] Figure 8 and supporting information Table S2 indicate that the individual forcing values needed to trigger retreat in combined sub-ice-shelf melting, sea level, and ice temperature forced experiments can be small in comparison to single-forced experiments (supporting information Table S1). For example, although sea-level does not drive retreat on its own unless it increases by around 135 m, retreat can begin between 5 and 55 m of sea level rise when ocean-driven melt rates are increased either gradually or rapidly (Figure 8). The forcing “space” within which retreat occurs (Figure 8) indicates potential limits of external change that may have driven deglaciation and is consistent with the idea of a critical threshold being required in order to initiate retreat, with forcings acting additively. For example, if ice temperature is warmed by approximately 7°C , the M_{max} required to induce retreat may be as little as 10 m yr^{-1} , and if sea level rose by approximately 40 m, an M_{max} of around 25 m yr^{-1} could be enough to trigger retreat. We note that the rate of increase in forcing is of secondary importance, affecting timescales of retreat-rate evolution, compared to the absolute additive magnitude in forcing that determines whether the grounding line begins to retreat in the first place. The triple-forced simulations (Figure 7f) produce similar patterns and rates of retreat as double-forced experiments but do so under smaller magnitudes of forcing (supporting information Table S2).

4.4. Set 4: Nonlinear Climate and Water Depth Evolution

[47] The results of these model experiments (Figure 9) indicate that despite including nonlinear ice temperature and

Figure 7. Modeled grounding-line retreat patterns under multiple linear forcings (supporting information Table S2). (a) Ice-temperature and sea-level forced models indicating that without some increase in ice temperature, the sea-level change is not readily felt and that sea-level rise would need to be significant to induce rapid retreat; (b) Ice temperature and melt-rate forced models showing that along with minimal ice temperature increases, retreat can be induced by enhancing melting beneath the ice shelf but that the model becomes less sensitive as melt rates increase; (c) Ice-temperature and ice-shelf debuttressing forced models showing that loss of buttressing is effective when small changes in ice temperature also occur; (d) Water depth and sub-ice-shelf melt rate forced models illustrating that once melt rates become significant, rising sea levels become less important for retreat speed; (e) Water depth and ice-shelf debuttressing forced models illustrating the ineffective nature of this combination of mechanisms for forcing full retreat. (f) Triple-forced experiments suggesting that even when multiple processes operate, the overall speeds and patterns of retreat can be very similar and are generally slower than the chronology for Marguerite Bay (Figure 2).

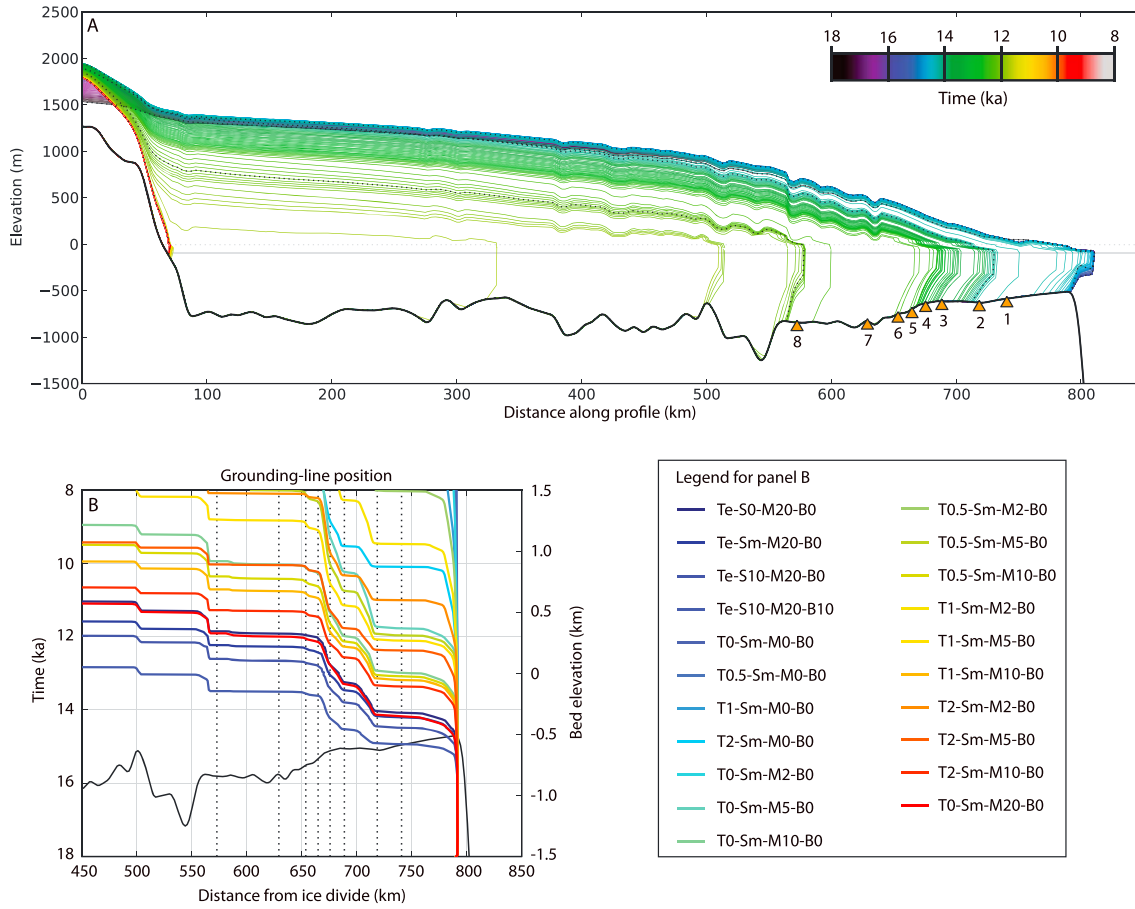


Figure 9. Nonlinearly forced model results. (a) Modeled ice surface evolution of experiment Te-Sm-M20-B0 forced using scaled and shifted EDC temperature fluctuations, a modeled sea-level history (Figure 4e), a maximum melt rate beneath the ice shelf which increases linearly at $20 \text{ m yr}^{-1} \text{ kyr}^{-1}$, and constant ice-shelf buttressing conditions (supporting information Table S2). Ice surface profiles are given every 250 years (colored lines) with 2 kyr isochrones (dashed black lines). The MBIS topography is shown by the solid black line, and GZWs 1–8 (Figure 2) are denoted by orange triangles. Note that only 10 kyr of model time are shown. Onset of retreat occurs as the sea level begins to increase and continues during the period of rapid sea-level rise (Figure 4e). (b) Modeled grounding-line retreat patterns indicating that the retreat pattern is not strongly controlled by fluctuations in the nonlinear forcings.

relative sea-level forcing patterns, the locations of modeled speedups versus slowdowns in grounding-line retreat rate do not change significantly in comparison to the linearly driven experiments. For example, MBIS grounding-line evolution and thinning patterns for the response of experiment Te-Sm-M20-B0 (Figure 9) to fluctuating ice temperature and modeled sea-level history [Peltier, 2004; Masson-Delmotte *et al.*, 2010] are not significantly different from those in linearly forced experiment T0-S0-M20-B0 (Figure 5). This indicates that both the recorded and modeled MBIS retreat patterns are consistent with the regional sea-level history and with the possible fluctuations in temperature that occurred following the LGM. Retreat begins in the EPICA-forced experiments between 15.3 and 14.6 ka and in the modeled sea-level forced experiments between 14.8 and 8.5 ka (supporting information Table S2). The imposition of a relative sea-level history (Figure 4e) does accelerate retreat, particularly as the grounding line passes into the steepest part of the reverse-sloping bed. The largest acceleration is concomitant with a rapid sea-level rise generated, for example, by a meltwater pulse. Retreat

continues during the period of the fastest increase in sea level and prolonged warming. However, minor climatic, and thus ice temperature, cooling events do not generate substantial readvances within the overall retreat phase due to their short-term nature.

5. Discussion

5.1. Width Control on Ice-Stream Retreat Rates

[48] Although external forcing is important for initiating and driving retreat, the consistent responses simulated in our linear and nonlinear experiments clearly indicate that local topographic conditions controlled retreat-rate patterns of the ice stream. Consistent with the geomorphic record, retreat is highly nonlinear, and the addition of a laterally buttressing ice shelf improves the data-model consistency compared to Jamieson *et al.* [2012]. As well as the importance of basal topography for controlling retreat rates, we confirm the importance of enhanced lateral drag (Figure 5b) as a buttressing mechanism which slows retreat in the more

constricted portions of the cross-shelf trough. Lateral drag is 20–30% higher around the steep reverse-sloped bed of the ice stream when compared to adjacent areas upstream or downstream (Figure 5). This means that when the grounding line retreats into such narrow areas of the trough, the ice flux required for maintaining a stable grounding line is reduced. This acts to reduce mass loss, and thus, ice-stream retreat rates. Hence, a narrowing trough in the upstream direction could theoretically pause grounding-line retreat while ice surface thinning continues. Furthermore, ice-surface steepening (Figures 5 and 9) is generated in convergent topographies as a result of enhanced lateral drag. Therefore, for a given rate of surface thinning or sea-level rise at the grounding line, the grounding line will retreat more slowly than would be possible if the ice-surface slope were not steepened [O’Neel et al., 2005].

[49] Our experiments produce slower grounding-line retreat rates across parts of the steep reverse bed slope than over shallower sloped regions. This suggests that ice streams in areas of steeply reverse-sloping topography are not always susceptible to rapid collapse [Weertman, 1974; Thomas, 1979; Schoof, 2007]. Instead of considering the stabilizing/destabilizing influence of topography solely in the vertical direction where it controls water depth in marine settings [Powell, 1991], our simulations indicate that assessments of ice-stream behavior must also consider variations in ice-stream width. Furthermore, ice streams which are laterally buttressed by an ice shelf may be particularly responsive to changes in trough width [Goldberg et al., 2009; Gudmundsson et al., 2012; Gudmundsson, 2013]. The importance of trough width in modulating retreat rates is also supported by observations and models in other settings including tidewater outlet glaciers in Alaska, Greenland and synthetic topographic settings [Warren and Glasser, 1992; O’Neel et al., 2005; Carr et al., 2013; Enderlin et al., 2013a] and in ice streams such as the Pine Island Glacier, where steep ice-surface slopes appear to correspond to reduced grounding-line retreat rates across a reverse-sloping bed during simulations of future ice-stream behavior [Gladstone et al., 2012].

5.2. Relative Importance of Forcing Mechanisms

[50] Many of the model experiments presented here are driven using magnitudes and/or durations of forcing that are, on average, higher than can be expected for Marguerite Bay during the last deglaciation (e.g., sea-level rise >30 m for >3 kyr, sub-ice-shelf melt rates >40 m yr⁻¹, or ice temperature increases by >2.5°C for >8 kyr). However, the range of scenarios tested allows a wider exploration of sensitivities which is important in light of the uncertainty about the pre-retreat ice-stream configuration. The single forcing experiments identify a very clear threshold behavior regarding the magnitude of forcing required to initiate retreat from the continental shelf edge. Onset of retreat appears to be controlled by reaching a critical threshold in sea-level rise, ocean-driven melting, or climatic (ice temperature) warming. This is consistent with the theory that the grounding line is stable at the shelf edge as long as ice flux at the grounding line remains below a critical level [Schoof, 2007]. However, all of these individually forced thresholds are unrealistically high, with melt rates being 3 times larger than those which occur in the extreme interglacial forcing of Pollard and DeConto [2009], sea level being significantly higher than the known regional highstand [Bentley et al., 2005], and ice

temperature being as warm as the modern mean annual air temperature threshold for ice-shelf instability on the AP [Cook and Vaughan, 2010].

[51] Although the scales of forcing are therefore important, the rate of forcing change appears to be of secondary significance for initiating retreat. Our sensitivity exploration suggests that sustained, rather than sudden, changes most likely initiated and then sustained retreat. Our experiments suggest that step forcing is generally less effective because the upstream portion of the ice stream is responsive enough to react to accelerate ice flux to the grounding line thereby allowing it to remain stable despite “shocks” to the system. There is also enough upstream ice to continue supplying the grounding line with ice, even though the shock may push the ice stream into negative mass balance.

[52] The large magnitude of individual forcings required to initiate retreat from the continental shelf edge suggests that a combination of processes drove the onset and continuation of retreat. Within the plausible range of forcings, our experiments suggest that the MBIS is more sensitive to forcing factors that include accelerations in melting at the ice-ocean boundary than to nonmelt combinations. This is supported by micropaleontological analyses documenting the advection of warm water masses onto the AP shelf and driving retreat [Kilfeather et al., 2011]. Retreat patterns simulated here fit more closely with the geophysical and geological data than previous work, which did not include an ice shelf [Jamieson et al., 2012], in that retreat slowdowns occur more often on the steepest part of the reverse-sloped bed when an ice shelf is present and in that their locations more closely correspond with those of the GZWs. In addition, experiments incorporating gradual or immediate ice-shelf debuttressing during retreat result in a slightly poorer spatial correspondence in the vicinity of GZW 2 (supporting information Tables S1 and S2 and Figures 7c and 7e). The implication is that an ice shelf was probably present and intact during post-LGM retreat in Marguerite Trough, at least while the grounding line passed over the sites of the GZWs. Lateral drag from the ice shelf enables the grounding line to be buttressed even when it has retreated inland of the trough narrowing. For example, with a 10 km long ice shelf, the narrowing would exert influence on the grounding line while it lies within 10 km upstream. This may have provided the time for sediment to begin accumulating at the grounding line, seeding the growth of the GZWs.

5.3. Model Limitations

[53] Our modeling indicates that onset of ice-stream retreat occurs when a threshold in forcing is crossed. This is consistent with crossing a critical ice flux threshold required for stability at the grounding line, which is heavily dependent upon the geometry of the bed at the shelf edge [Schoof, 2007]. Therefore, alongside the magnitude of the change in forcing, the timing of retreat onset (or whether the ice stream retreats at all) depends critically on the initial LGM ice condition applied in our model. In particular, the proximity of the initial ice-stream flux to the critical threshold for unstable retreat controls how easily retreat will be initiated. Consequently, there are a number of limitations in the initial model configuration that may impact the model response to threshold conditions.

[54] First, our initial ice stream is too thick in the inland portion of the trough. Cosmogenic nuclide exposure ages from Alexander Island, where it bounds George VI Sound

(Figure 1), suggest that the ice stream surface had lowered to below 650 m above sea level (asl) by 25.5 ka and below 600 m asl by 17.3 ka [cf. *Bentley et al.*, 2006, 2011]. This thinning preceded the retreat of the grounding line from the continental shelf edge (Figure 2). However, for an LGM ice surface of 650 m elevation at Alexander Island, ice surface gradients are too low to produce enough ice flux to enable the grounding-line to maintain its position at the continental shelf edge. Instead, we achieve a stable LGM grounding line at the edge of the continental shelf with an ice surface at approximately 1250 m asl near Alexander Island. Assuming the exposure age data are robust, this discrepancy is problematic because if ice discharge is greater than total accumulation, the ice volume stored upstream determines the timescale over which ice can be delivered to the grounding line. This volume is partly controlled by constrictions in trough width because they generate steep ice-surface slopes behind which total upstream ice volume is highly sensitive. Therefore, our retreat may be too slow as a result of slightly exaggerated ice volumes in the upper trough. In addition, the ability of the upstream ice to respond to changes at the grounding line controls the rate of ice delivery to the terminus. In general, the upstream propagation of flow acceleration and thinning is strongly controlled by ice velocity and surface slope [*Payne et al.*, 2004]. Due to the relatively wide ice stream inland, this responsiveness is more strongly controlled by the strength of the bed than by lateral buttressing. Additional measurements of bed strength would therefore help improve the configuration of the initial ice-stream model.

[55] Second, factors such as external forcing conditions at the LGM remain poorly constrained. Therefore, our ability to predict the “absolute timing” of retreat remains uncertain such that our modeling study concentrates on the rate and pattern of retreat relative to the onset of retreat from the continental shelf edge. The issue of underconstrained three-dimensional LGM ice-sheet configurations is typical around Antarctica and other glaciated margins and may pose a general problem of predicting onset of retreat from the continental shelf. The problem mainly arises because distances between the LGM grounding-line position and the location of data constraining the paleo-ice sheet surface elevation are often hundreds of kilometers, meaning that seemingly minor discrepancies in modeled ice-stream surface slopes can result in significant uncertainties in ice thickness.

[56] Finally, we consider that although our modeled pattern of width-controlled variability in retreat rate is likely to be robust, the timescales of retreat may be too slow. As already discussed, this may result from the imposition of thicker inland ice in George VI Sound. However, it may also be the consequence of initiating our retreat simulations from an unintentionally overstabilized configuration or because the model physics or parameterizations themselves induce a less rapid response than occurred in reality. In the former case, it is likely that the LGM position was part of a transient response to cooling and that the ice stream never reached a stable “steady state” at the LGM. This transience is supported by the apparent contrast between terrestrial and offshore retreat ages, which suggests ice-surface thinning prior to grounding-line retreat [*Pope and Anderson*, 1992; *Bentley et al.*, 2006, 2011; *Kilfeather et al.*, 2011]. We acknowledge, therefore, that because of the limitation of simulating an initial ice stream with thinner ice in the upstream region, the model may overestimate the resilience to rapid, large-scale

forcing events. In the latter case, the model reliance upon a simple parameterization of lateral stress which is calculated as a function of ice velocity, thickness, and width, may impact the simulated retreat response. We suspect that this limitation is retarding retreat rates in our model because it may be partly responsible for the presence of overly thick ice in the upstream trough. Likewise, as found by *Enderlin et al.* [2013b], the model dependency upon parameters, for example, in calculating shear stresses, may influence the speed of grounding-line retreat, but we do not believe these model limitations will substantially affect the spatial pattern of retreat slowdowns or accelerations. However, further investigations using three-dimensional higher-order models that fully resolve lateral shear stresses [e.g., *Gudmundsson et al.*, 2012; *Pattyn et al.*, 2012] will help to refine our understanding of the impact that topographic width has upon ice-stream grounding-line retreat rates. The future application of such models should be combined with more extensive bathymetric surveying in Marguerite Bay to better define the trough geometry and reduce uncertainty in understanding the importance of width.

5.4. Implications for Understanding Past, Present, and Future Ice Stream Retreat

[57] Our modeling has implications for interpreting the rates of past, present, and future ice-stream retreat. We produce centennial- to millennial-scale slowdowns in retreat at the locations of GZWs identified from marine geophysical mapping [*Ó Cofaigh et al.*, 2002, 2005; *Dowdeswell et al.*, 2008; *Ó Cofaigh et al.*, 2008]. Our modeling suggests that such apparently slow retreat rates viewed over a short period may obscure a longer-term, larger-scale pattern of retreat which would be crucial for conditioning subsequent grounding-line retreat rates.

[58] The experiments presented here also indicate that significant contrasts in behavior might be expected between adjacent but topographically distinct catchments. The implication is that despite regional- or global-scale forcing, retreat patterns are likely to be different because of the unique topographic settings of individual ice streams. This provides a potential explanation for contrasting post-LGM temporal and spatial retreat patterns throughout Antarctica and in particular between adjacent ice streams on the Antarctic Peninsula [*Livingstone et al.*, 2012]. Indeed, the strong dependence of ice-stream dynamics upon topography suggests that regional or global environmental changes should induce asynchronous, topographically predefined patterns of retreat with even small-scale variations in topography influencing retreat patterns. Consequently, the prediction of future relative-retreat rates depends on the availability of high-quality three-dimensional bed data at, and upstream of, modern grounding lines [*Durand et al.*, 2011] as well as observations of modern rates of melting beneath ice shelves, evolving accumulation patterns and ice velocities, and subglacial sediment and hydrology conditions.

6. Conclusions

[59] Using a model of ice-stream and grounding-line behavior adapted for long-term simulations, we explore the sensitivity of post-LGM ice-stream retreat in Marguerite Bay, Antarctic Peninsula, to a range of simple forcing parameters and histories. The dimensions of a cross-shelf trough and the distribution of linear subglacial landforms mapped from marine geophysical data control the model geometry. Modeled retreat

patterns are compared against the distribution of a series of grounding-zone wedges that independently record grounding-line position during the overall phase of retreat. Our key findings are:

[60] 1. Grounding-line retreat rates are highly nonlinear, even under linear forcing, and consistently slow down in close proximity to mapped grounding-zone wedges. The marine geophysical data and the dynamic models are in sufficient agreement to conclude that although external forcing is important for initiating retreat, the rates of retreat are strongly controlled by the individual geometry of the topography through which the ice stream flows.

[61] 2. Our analysis indicates that enhanced lateral drag, associated with narrowing of the ice stream within its trough, enables the retreat-rate slowdowns to occur, even on steeply reverse-sloping beds. This demonstrates that reverse-sloping beds do not always induce rapid grounding-line retreat.

[62] 3. We find that the onset of retreat from the continental shelf edge depends on a threshold in forcing magnitude being crossed. However, the rate of change of the forcing only has a significant influence on the subsequent retreat rates, in particular where the ice-stream trough narrows.

[63] 4. We find only minor enhancements in data-model fit when we force retreat using a nonlinear ice-temperature or sea-level forcing. Furthermore, modeled retreat is insensitive to events, such as meltwater pulses, and instead requires a sustained forcing throughout the duration of retreat to drive full deglaciation. Given model limitations, a three-dimensional full-stress model is required to assess whether this conclusion is robust.

[64] 5. Sensitivity analysis suggests that the MBIS was most susceptible to ocean-driven melting beneath the ice shelf but that retreat was at least partially forced by other external processes. Nevertheless, rapid retreat is only induced when ocean-driven melt conditions are combined with a relatively large sea-level rise or ice-temperature increase.

[65] 6. Stronger agreement between the modeled retreat pattern and the geomorphological evidence occurs when ice-shelf buttressing continues during grounding-line retreat across the outer and middle continental shelves. We therefore infer that, following the LGM, an ice shelf was present during periods of GZW deposition.

[66] 7. The responsiveness and volume of the upstream ice controls how fast the grounding line can retreat. In the case of the MBIS, which is largely underlain by soft sediment and therefore offers minimal basal resistance, the transfer of ice to the grounding line from upstream can be rapid. This allows the grounding line to maintain its position under enhanced dynamic thinning conditions until the upstream ice volume is sufficiently depleted that ice cannot not be supplied any longer at the rate required for stability.

[67] 8. Our sensitivity test results imply that as a result of differing lateral and vertical trough topography, adjacent ice streams would be expected to show different spatial and temporal retreat behaviors, even under identical regional or global forcing.

[68] 9. Future assessments and simulations of ice-stream behavior and ice-sheet stability require detailed three-dimensional topographic data. This will identify variations in width and depth upstream of modern grounding lines, allowing the assessment of the rate of ice discharge to the ocean and plausible rates and timescales of mass loss and grounding-line retreat.

[69] 10. Predictive models of ice-stream behavior often begin from a modern steady state configuration. However, by using data constraining the long-term ice stream retreat history, the initiation of more realistic transitional modern states may be possible and may enable wider exploration of future ice stream retreat patterns.

[70] **Acknowledgments.** This work was funded by Natural Environment Research Council (NERC) UK standard grants NE/G015430/1 (Vieli) and NE/G018677/1 (Hillenbrand) and NERC Fellowship grant NE/J018333/1 (Jamieson). Underlying data are available by request to Jamieson. We are grateful to Pippa Whitehouse for providing a local ICE-5G-based sea-level history, to Tony Payne and Richard Hindmarsh for the valuable discussions on the numerical modeling, and to Julian Dowdeswell for contributing parts of the underlying marine geophysical data. We acknowledge the efforts of Neil Ross, Mathieu Morlighem, Poul Christoffersen, and an anonymous reviewer for their constructive comments which helped improve this manuscript.

References

- Alley, R. B., D. D. Blankenship, C. R. Bentley, and S. T. Rooney (1986), Deformation of till beneath ice stream B, West Antarctica, *Nature*, *322*(6074), 57–59.
- Alley, R. B., S. Anandakrishnan, T. K. Dupont, B. R. Parizek, and D. Pollard (2007), Effect of sedimentation on ice-sheet grounding-line stability, *Science*, *315*(5820), 1838–1841.
- Anandakrishnan, S., and R. B. Alley (1997), Stagnation of ice stream C, West Antarctica by water piracy, *Geophys. Res. Lett.*, *24*(3), 265–268.
- Anandakrishnan, S., D. E. Voigt, R. B. Alley, and M. A. King (2003), Ice stream D flow speed is strongly modulated by the tide beneath the Ross Ice Shelf, *Geophys. Res. Lett.*, *30*(7), 1361, doi:10.1029/2002GL016329.
- Arthern, R. J., D. P. Winebrenner, and D. G. Vaughan (2006), Antarctic snow accumulation mapped using polarization of 4.3-cm wavelength microwave emission, *J. Geophys. Res.*, *111*, D06107, doi:10.1029/2004JD005667.
- Bamber, J. L., D. G. Vaughan, and I. Joughin (2000), Widespread complex flow in the interior of the Antarctic Ice Sheet, *Science*, *287*(5456), 1248–1250.
- Benn, D. I., N. R. J. Hulton, and R. H. Mottram (2007), ‘Calving laws’, ‘sliding laws’, and the stability of tidewater glaciers, *Ann. Glaciol.*, *46*, 123–130.
- Bentley, M. J., D. A. Hodgson, J. A. Smith, and N. J. Cox (2005), Relative sea level curves for the South Shetland Islands and Marguerite Bay, Antarctic Peninsula, *Quat. Sci. Rev.*, *24*(10–11), 1203–1216.
- Bentley, M. J., C. J. Fogwill, P. W. Kubik, and D. E. Sugden (2006), Geomorphological evidence and cosmogenic ¹⁰Be/²⁶Al exposure ages for the Last Glacial Maximum and deglaciation of the Antarctic Peninsula Ice Sheet, *Geol. Soc. Am. Bull.*, *118*(9–10), 1149–1159.
- Bentley, M. J., J. S. Johnson, D. A. Hodgson, T. Dunai, S. P. H. T. Freeman, and C. Ó Cofaigh (2011), Rapid deglaciation of Marguerite Bay, western Antarctic Peninsula in the Early Holocene, *Quat. Sci. Rev.*, *30*(23–24), 3338–3349.
- Bougamont, M., S. Tulaczyk, and I. Joughin (2003), Response of subglacial sediments to basal freeze-on 2. Application in numerical modeling of the recent stoppage of Ice Stream C, West Antarctica, *J. Geophys. Res.*, *108*(B4), 2223, doi:10.1029/2002JB001936.
- Briner, J. P., A. C. Bini, and R. S. Anderson (2009), Rapid early Holocene retreat of a Laurentide outlet glacier through an Arctic fjord, *Nat. Geosci.*, *2*(7), 496–499.
- Carr, J. R., A. Vieli, and C. R. Stokes (2013), Influence of sea ice decline, atmospheric warming, and glacier width on marine-terminating outlet glacier behavior in northwest Greenland at seasonal to interannual timescales, *J. Geophys. Res. Earth Surface*, *118*, 1210–1226, doi:10.1002/jgrf.20088.
- Cook, A. J., and D. G. Vaughan (2010), Overview of areal changes of the ice shelves on the Antarctic Peninsula over the past 50 years, *Cryosphere*, *4*, 77–98.
- Dowdeswell, J. A., and E. M. G. Fugelli (2012), The seismic architecture and geometry of grounding-zone wedges formed at the marine margins of past ice sheets, *Geol. Soc. Am. Bull.*, *124*(11–12), 1750–1761.
- Dowdeswell, J. A., D. Ottesen, J. Evans, C. Ó Cofaigh, and J. B. Anderson (2008), Submarine glacial landforms and rates of ice-stream collapse, *Geology*, *36*(10), 819–822.
- Dupont, T. K., and R. B. Alley (2005), Assessment of the importance of ice-shelf buttressing to ice-sheet flow, *Geophys. Res. Lett.*, *32*, L04503, doi:10.1029/2004GL022024.
- Durand, G., O. Gagliardini, L. Favier, T. Zwinger, and E. le Meur (2011), Impact of bedrock description on modeling ice sheet dynamics, *Geophys. Res. Lett.*, *38*, L20501, doi:10.1029/2011GL048892.
- Enderlin, E. M., I. M. Howat, and A. Vieli (2013a), High sensitivity of tidewater outlet glacier dynamics to shape, *Cryosphere*, *7*, 1007–1015.
- Enderlin, E. M., I. M. Howat, and A. Vieli (2013b), The sensitivity of flowline models of tidewater glaciers to parameter uncertainty, *Cryosphere*, *7*, 1579–1590.

- Fahnestock, M. A., T. A. Scambos, R. A. Bindschadler, and G. Kvaran (2000), A millennium of variable ice flow recorded by the Ross Ice Shelf, Antarctica, *J. Glaciol.*, *46*(155), 652–664.
- Fairbanks, R. G. (1989), A 17,000-year glacio-eustatic sea level record: Influence of glacial melting rates on the Younger Dryas event and deep-ocean circulation, *Nature*, *342*, 637–642.
- Fretwell, P., et al. (2013), Bedmap2: Improved ice bed, surface and thickness datasets for Antarctica, *Cryosphere*, *7*, 375–393.
- Gladstone, R. M., V. Lee, J. Rougier, A. J. Payne, H. Hellmer, A. Le Brocq, A. Shepherd, T. L. Edwards, J. Gregory, and S. L. Cornford (2012), Calibrated prediction of Pine Island Glacier retreat during the 21st and 22nd centuries with a coupled flowline model, *Earth Planet. Sci. Lett.*, *333–334*, 191–199.
- Glen, J. W. (1955), The creep of polycrystalline ice, *Proc. R. Soc. London Ser. A*, *228*, 519–387.
- Goldberg, D., D. M. Holland, and C. Schoof (2009), Grounding line movement and ice shelf buttressing in marine ice sheets, *J. Geophys. Res.*, *114*, F04026, doi:10.1029/2008JF001227.
- Graham, A. G. C., F. O. Nitsche, and R. D. Larter (2011), An improved bathymetry compilation for the Bellingshausen Sea, Antarctica, to inform ice-sheet and ocean models, *Cryosphere*, *5*, 95–106.
- Gudmundsson, G. H. (2013), Ice-shelf buttressing and the stability of marine ice sheets, *Cryosphere*, *7*, 647–655.
- Gudmundsson, G. H., J. Krug, G. Durand, L. Favier, and O. Gagliardini (2012), The stability of grounding lines on retrograde slopes, *Cryosphere*, *6*, 1497–1505.
- Heroy, D. C., and J. B. Anderson (2007), Radiocarbon constraints on Antarctic Peninsula Ice Sheet retreat following the Last Glacial Maximum (LGM), *Quat. Sci. Rev.*, *26*(25–28), 3286–3297.
- Hindmarsh, R. C. A. (2006), The role of membrane-like stresses in determining the stability and sensitivity of the Antarctic ice sheets: Back pressure and grounding line motion, *Philos. Trans. R. Soc. London Ser. A*, *364*, 1733–1767.
- Holland, P. R., A. Jenkins, and D. M. Holland (2010), Ice and ocean processes in the Bellingshausen Sea, Antarctica, *J. Geophys. Res.*, *115*, C05020, doi:10.1029/2008JC005219.
- Jacobel, R. W., T. A. Scambos, N. A. Nereson, and C. F. Raymond (2000), Changes in the margin of Ice Stream C, Antarctica, *J. Glaciol.*, *46*, 102–110.
- Jacobs, S. S., A. Jenkins, C. F. Guillivi, and P. Dutrieux (2011), Stronger ocean circulation and increased melting under Pine Island Glacier ice shelf, *Nat. Geosci.*, *4*, 519–523.
- Jamieson, S. S. R., A. Vieli, S. J. Livingstone, C. Ó Cofaigh, C. Stokes, C.-D. Hillenbrand, and J. A. Dowdeswell (2012), Ice-stream stability on a reverse bed slope, *Nat. Geosci.*, *5*(11), 799–802.
- Jenkins, A., and S. S. Jacobs (2008), Circulation and melting beneath George VI Ice Shelf, Antarctica, *J. Geophys. Res.*, *113*, C04013, doi:10.1029/2007JC004449.
- Joughin, I., S. Tulaczyk, R. Bindschadler, and S. F. Price (2002), Changes in west Antarctic ice stream velocities: Observation and analysis, *J. Geophys. Res.*, *107*(B11), 2289, doi:10.1029/2001JB001029.
- Joughin, I., E. Rignot, C. E. Rosanova, B. K. Lucchitta, and J. Bohlander (2003), Timing of recent accelerations of Pine Island Glacier, Antarctica, *Geophys. Res. Lett.*, *30*(13), 1706, doi:10.1029/2003GL017609.
- Jouzel, J., et al. (2007), Orbital and millennial Antarctic climate variability over the past 800,000 years, *Science*, *317*(5839), 793–796.
- Kilfeather, A. A., C. Ó Cofaigh, J. M. Lloyd, J. A. Dowdeswell, S. Xu, and S. G. Moreton (2011), Ice-stream retreat and ice-shelf history in Marguerite Trough, Antarctic Peninsula: Sedimentological and foraminiferal signatures, *Geol. Soc. Am. Bull.*, *123*(5-6), 997–1015.
- Le Brocq, A. M., A. J. Payne, and A. Vieli (2010), An improved Antarctic dataset for high resolution numerical ice sheet models (ALBMAP v1), *Earth Syst. Sci. Data*, *2*, 247–260.
- Livingstone, S. J., C. Ó Cofaigh, C. R. Stokes, C.-D. Hillenbrand, A. Vieli, and S. S. R. Jamieson (2012), Antarctic palaeo-ice streams, *Earth Sci. Rev.*, *111*(1–2), 90–128.
- Livingstone, S. J., C. Ó Cofaigh, C. R. Stokes, C. D. Hillenbrand, A. Vieli, and S. S. R. Jamieson (2013), Glacial geomorphology of Marguerite Bay Palaeo-Ice stream, western Antarctic Peninsula, *J. Maps*, *9*(4), 558–572.
- Lytche, M., D. G. Vaughan, and B. Consortium (2001), BEDMAP: A new ice thickness and subglacial topographic model of Antarctica, *J. Geophys. Res.*, *106*, 11,335–11,352.
- Masson-Delmotte, V., et al. (2010), EPICA Dome C record of glacial and interglacial intensities, *Quat. Sci. Rev.*, *29*(1–2), 113–128.
- Nick, F. M., A. Vieli, I. M. Howat, and I. Joughin (2009), Large-scale changes in Greenland outlet glacier dynamics triggered at the terminus, *Nat. Geosci.*, *2*, 110–114.
- Nick, F. M., C. J. Van Der Veen, A. Vieli, and D. I. Benn (2010), A physically based calving model applied to marine outlet glaciers and implications for the glacier dynamics, *J. Glaciol.*, *56*(199), 781–794.
- Nick, F. M., A. Vieli, M. L. Andersen, I. Joughin, A. J. Payne, T. L. Edwards, F. Pattyn, and R. S. W. van de Wal (2013), Future sea-level rise from Greenland's main outlet glaciers in a warming climate, *Nature*, *497*(7448), 235–238.
- Ó Cofaigh, C., C. J. Pudsey, J. A. Dowdeswell, and P. Morris (2002), Evolution of subglacial bedforms along a paleo-ice stream, Antarctic Peninsula continental shelf, *Geophys. Res. Lett.*, *29*(8), 1199, doi:10.1029/2001GL014488.
- Ó Cofaigh, C., J. A. Dowdeswell, C. S. Allen, J. F. Hiemstra, C. J. Pudsey, J. Evans, and D. J. A. Evans (2005), Flow dynamics and till genesis associated with a marine-based Antarctic palaeo-ice stream, *Quat. Sci. Rev.*, *24*(5–6), 709–740.
- Ó Cofaigh, C., J. A. Dowdeswell, J. Evans, and R. D. Larter (2008), Geological constraints on Antarctic palaeo-ice-stream retreat, *Earth Surf. Processes Landforms*, *33*(4), 513–525.
- O'Neel, S., W. T. Pfeffer, R. Krimmel, and M. F. Meier (2005), Evolving force balance at Columbia Glacier, Alaska, during its rapid retreat, *J. Geophys. Res.*, *110*, F03012, doi:10.1029/2005JF000292.
- Pattyn, F., and A. J. Payne (2006), Ice Sheet Model Intercomparison Project: Benchmark Experiments for Higher-Order Ice Sheet Models (ISMIP-HOM), *Geophys. Res. Abstr.*, *8*, 04,969.
- Pattyn, F., et al. (2012), Results of the Marine Ice Sheet Model Intercomparison Project, *MISMIP, Cryosphere*, *6*, 573–588.
- Payne, A. J., A. Vieli, A. P. Shepherd, D. J. Wingham, and E. Rignot (2004), Recent dramatic thinning of largest West Antarctic ice stream triggered by oceans, *Geophys. Res. Lett.*, *31*, L23401, doi:10.1029/2004GL021284.
- Peltier, W. R. (2004), Global glacial isostasy and the surface of the ice-age Earth: The ICE-5G (VM2) model and GRACE, *Annu. Rev. Earth Planet. Sci.*, *32*, 111–149.
- Pollard, D., and R. DeConto (2009), Modelling West Antarctic ice sheet growth and collapse through the past five million years, *Nature*, *458*, 329–332.
- Pope, P. G., and J. B. Anderson (1992), Late Quaternary glacial history of the northern Antarctic Peninsula's western continental shelf: Evidence from the marine record, *Antarct. Res. Ser.*, *57*, 63–91.
- Powell, R. D. (1991), Grounding-line systems as second-order controls on fluctuations of tidewater termini of temperate glaciers, in *Glacial Marine Sedimentation: Paleoclimatic Significance*, edited by J. B. Anderson and G. M. Ashley, pp. 75–94, Geological Society of America, Special Paper, Boulder.
- Powell, R. D., and E. Domack (1995), Modern glaciomarine environments, in *Lacial Environments: Volume 1. Modern Glacial Environments: Processes, Dynamics and Sediments*, edited by J. Menzies, pp. 445–486, Butterworth-Heinemann, Oxford.
- Price, S. F., H. Conway, E. D. Waddington, and R. A. Bindschadler (2008), Model investigations of inland migration of fast-flowing outlet glaciers and ice streams, *J. Glaciol.*, *54*(184), 49–60.
- Pritchard, H. D., R. J. Arthern, D. G. Vaughan, and L. A. Edwards (2009), Extensive dynamic thinning on the margins of the Greenland and Antarctic ice sheets, *Nature*, *461*(7266), 971–975.
- Rignot, E., and S. S. Jacobs (2002), Rapid bottom melting widespread near Antarctic Ice Sheet grounding lines, *Science*, *296*, 2020–2023.
- Schoof, C. (2007), Ice sheet grounding line dynamics: Steady states, stability, and hysteresis, *J. Geophys. Res.*, *112*, F03S28, doi:10.1029/2006JF000664.
- Shepherd, A., D. Wingham, and E. Rignot (2004), Warm ocean is eroding West Antarctic Ice Sheet, *Geophys. Res. Lett.*, *31*, L23402, doi:10.1029/2004GL021106.
- Siegert, M. J., and A. J. Payne (2004), Past rates of accumulation in central West Antarctica, *Geophys. Res. Lett.*, *31*, L12403, doi:10.1029/2004GL020290.
- Siegert, M. J., A. J. Payne, and I. Joughin (2003), Spatial stability of Ice Stream D and its tributaries, West Antarctica, revealed by radio-echo sounding and interferometry, *Ann. Glaciol.*, *37*, 377–382.
- Smith, D. A., E. E. Hofmann, J. M. Klinck, and C. M. Lascara (1999), Hydrography and circulation of the West Antarctic Peninsula Continental Shelf, *Deep Sea Res. Part 1*, *46*(6), 925–949.
- Thomas, R. H. (1979), The dynamics of marine ice sheets, *J. Glaciol.*, *24*(90), 167–177.
- Thomas, R. H., and C. R. Bentley (1978), A model for Holocene retreat of the West Antarctic Ice Sheet, *Quatern. Res.*, *10*, 150–170.
- van der Veen, C. J., and I. M. Whillans (1996), Model experiments on the evolution and stability of ice streams, *Ann. Glaciol.*, *23*, 129–137.
- Vieli, A., and A. J. Payne (2005), Assessing the ability of numerical ice sheet models to simulate grounding line migration, *J. Geophys. Res.*, *110*, F01003, doi:10.1029/2004JF000202.
- Warren, C. R., and N. F. Glasser (1992), Contrasting response of South Greenland glaciers to recent climatic change, *Arct. Alp. Res.*, *24*(2), 124–132.
- Weertman, J. (1957), On the sliding of glaciers, *J. Glaciol.*, *3*, 33–38.
- Weertman, J. (1974), Stability of the junction of an ice sheet and an ice shelf, *J. Glaciol.*, *13*(67), 3–11.
- Whillans, I. M., and C. J. van der Veen (1997), The role of lateral drag in the dynamics of Ice Stream B, Antarctica, *J. Glaciol.*, *43*(144), 231–237.
- Wolff, E. W., et al. (2010), Changes in environment over the last 800,000 years from chemical analysis of the EPICA Dome C ice core, *Quat. Sci. Rev.*, *29*(1–2), 285–295.